

Change-points analysis for generalized integer-valued autoregressive model via minimum description length principle

Danshu Sheng¹, Dehui Wang^{1*}

Abstract This article considers the problem of modeling a class of nonstationary count time series using multiple change-points generalized integer-valued autoregressive (MCP-GINAR) processes. The minimum description length principle (MDL) is applied to study the statistical inference for the MCP-GINAR model, and the consistency results of the MDL model selection procedure are established respectively under the condition of known and unknown number of change-points. To find the “best” combination of the number of change-points, the locations of change-points, the order of each segment and its parameters, a genetic algorithm with simulated annealing is implemented to solve this difficult optimization problem. In particular, the simulated annealing process makes up for the precocious problem of the traditional genetic algorithm. Numerical results from simulation experiments and three examples of real data analyses show that the procedure has excellent empirical properties.

Keywords : GINAR(p) model · multiple change-points · minimum description length · genetic algorithm · simulated annealing

1 Introduction

Modeling and analysis of count time series have attracted a lot of attention over the last years. Since [Al-Osh and Alzaid \(1987\)](#) proposed the first order integer-valued autoregressive (INAR(1)) time series model based on binomial thinning operator ([Steutel and Van Harn \(1979\)](#)), modeling INAR-type models based on different thinning operators have become a common approach and have been widely used in many fields like epidemiology, social sciences, economics, life sciences and others. Furthermore, to make the integer-valued models based on thinning more flexible for practical purposes, [Latour \(1998\)](#) generalized the binomial thinning operator to a generalized thinning operator and proposed the following causal and stationary generalized integer-valued autoregressive (GINAR(p)) process,

¹School of Mathematics and Statistics, Liaoning University, Shenyang, China

*Corresponding author, E-mail: wangdehui@lnu.edu.cn

Definition 1 The GINAR(p) model $\{X_t\}_{t \geq 1}$ is defined by the following recursion

$$X_t = \sum_{k=1}^p \alpha_k \circ_G X_{t-k} + Z_t, \quad (1.1)$$

where $\alpha \circ_G X = \sum_{i=1}^X B_i$, $\{B_i\}$ is an independent identically distributed (i.i.d.) integer-valued random sequence with mean $\alpha \in (0, 1)$ and independent of non-negative integer-valued random variable X . $\{Z_t\}$ is a sequence of i.i.d. integer-valued random variables with mean γ and Z_t is not depending on past values of $\{X_s\}_{s < t}$.

Due to the flexibility and practicability of the GINAR models, a large quantity of articles focusing on the modeling and statistical inference for such models have arisen. For example, [Ristić et al. \(2009\)](#), [Nastić et al. \(2012\)](#), [Scotto et al. \(2018\)](#), [Barreto-Souza \(2019\)](#), and [Darolles et al. \(2019\)](#) considered the modeling of the INAR-type models to better handle the fitting problems. [Zheng et al. \(2006\)](#), [Silva and Silva \(2006\)](#), [Bu et al. \(2008\)](#) studied the parameter estimation for the GINAR(p) models. [Fernández-Fontelo et al. \(2016\)](#), [Fernández-Fontelo et al. \(2021\)](#), [Henderson and Rathouz \(2018\)](#), [Guan and Hu \(2022\)](#) and [Gourieroux and Jasiak \(2004\)](#) applied the INAR-type models to under-reported data, longitudinal data and insurance actuarial.

Note that the GINAR models are typically used to describe stationary processes, while it is well known that non-stationary processes are also a common phenomenon in statistics. Although complex non-stationary models have been developed in different fields, they are often difficult to explain. The concept of piecewise stationary models has become a popular method by dividing nonstationary data into several stationary parts. Among the different types of piecewise stationary models, the so-called multiple change-points (MCP) models have received special attention. Studies of change-points models date back to [Page \(1954, 1955\)](#). Since then, this topic has been of interest to statisticians and researchers in many other fields. Such as, in financial analysis, [Russell and Rambaccussing \(2019\)](#) identified inflation regime by detecting changes in the mean of a stationary process, in medicine, [Jong et al. \(2003\)](#) identified the presence of tumors by detecting breaks in the Array Genome sequence, in climatology, [Shi et al. \(2022\)](#) analyzed the causes of temperature changes by detecting structural changes in the Central England temperature series.

Based on different data types, the study of time series can be divided into continuous and count time series models. So far, many excellent articles, such as [Lee et al. \(2003\)](#), [Davis et al. \(2006\)](#), [Chan et al. \(2014\)](#), [Chen et al. \(2021\)](#), [Aue and Horváth \(2013\)](#), [Niu et al. \(2016\)](#), [Casini and Perron \(2018\)](#), [Truong et al. \(2020\)](#), just to name a few, have studied and reviewed methodological issues related to estimation, detection and computation for continuous time series models involving structural changes. In contrast, the research of count time series models involving structural changes is still mainly focused on the change-points detection. Such as, among others, [Kang and Lee \(2009\)](#), [Yu and Kim \(2020\)](#) and [Lee and Jo \(2022\)](#) considered the problem of testing for a parameter change in different types of INAR(1) models by taking advantage of the cumulative sum (CUSUM) test. [Diop](#)

and Kengne (2021a), Diop and Kengne (2022) constructed test statistics, which is based on Poisson quasi-maximum likelihood estimator of the parameters, to detect changes in the mean parameters of the generalized integer-valued models, and then used this procedure to detect changes in the number of epidemic cases. Chattopadhyay et al. (2021) considered the problem of change-point analysis for the INAR(1) model with time-varying covariates. Yu et al. (2022) applied the empirical likelihood ratio (ELR) test to uncover a structural change in INAR processes.

However, there is surprisingly little research on the change-points estimation of count time series. To task this, the main goal of this article is to introduce the following piecewise stationary model, multiple change-points generalized integer-valued autoregressive model (MCP-GINAR), to describe the common non-stationary processes in count time series, and then study its change-points estimation,

Definition 2 *The MCP-GINAR process with m change-points $\{X_t\}_{t=1}^n$ is defined by the recursion:*

$$X_t = \begin{cases} \alpha_{1,1} \circ_G X_{t-1,1} + \dots + \alpha_{p_1,1} \circ_G X_{t-p_1,1} + Z_{t,1}, & 0 < t \leq \tau_1, \\ \vdots \\ \alpha_{1,j} \circ_G X_{t-1,j} + \dots + \alpha_{p_j,j} \circ_G X_{t-p_j,j} + Z_{t,j}, & \tau_{j-1} < t \leq \tau_j, \\ \vdots \\ \alpha_{1,m} \circ_G X_{t-1,m} + \dots + \alpha_{p_m,m} \circ_G X_{t-p_m,m} + Z_{t,m}, & \tau_m < t \leq n, \end{cases} \quad (1.2)$$

where $\boldsymbol{\tau} = (\tau_1, \tau_2, \dots, \tau_m)$ denotes the vector of unknown locations of change-points, $\tau_0 = 0$ and $\tau_{m+1} = n$. Each change-points location τ_j is an integer between 1 and $n - 1$ inclusive and the change-points are ordered such that $\tau_{j_1} < \tau_{j_2}$ if, and only if, $j_1 < j_2$. The time series $\boldsymbol{x}_n = (X_1, X_2, \dots, X_n)$ can be written as

$$\boldsymbol{x}_n = (X_{1,1}, \dots, X_{n_1,1}, X_{1,2}, \dots, X_{n_2,2}, \dots, X_{1,j}, \dots, X_{n_j,j}, \dots, X_{1,m+1}, \dots, X_{n_{m+1},m+1}), \quad (1.3)$$

where $n_j = \tau_j - \tau_{j-1}$ for $j = 1, \dots, m + 1$ and $n = n_1 + n_2 + \dots + n_{m+1}$. In particular, the j -th piece $\{X_{t,j}\}_{t=1}^{n_j}$ of the series is modeled as an GINAR process (1.1) with order p_j ,

$$X_{t,j} = \alpha_{1,j} \circ_G X_{t-1,j} + \dots + \alpha_{p_j,j} \circ_G X_{t-p_j,j} + Z_{t,j}, \quad (1.4)$$

where “ \circ_G ” is defined in Definition 1, $\{Z_{t,j}\}$ is a sequence of i.i.d. random variables with mean $\gamma_j > 0$. $\boldsymbol{\theta}_j = (\alpha_{1,j}, \dots, \alpha_{p_j,j}, \gamma_j)$ is the parameter vector corresponding to this GINAR(p_j) process, which is assumed to be an interior point of the compact space $\Theta_j(p_j) = (0, +\infty) \times (0, 1)^{p_j}$.

For change-points estimation, we can regard it as a model selection problem. One common approach is to minimize a specific information criterion (IC) to select an optimal model. Given that our main focus is on estimating unknown parameters (the change-points number m , the change-points locations $\boldsymbol{\tau} = (\tau_1, \tau_2, \dots, \tau_m)$, the order of each segment GINAR process p_j and the corresponding parameter $\boldsymbol{\theta}_j = (\alpha_{1,j}, \dots, \alpha_{p_j,j}, \gamma_j)$) in the model (1.2), we apply

the minimum description length (MDL) principle of [Rissanen \(1989\)](#) to define a best-fitting model. MDL principle is designed to select a model that enables maximum compression of the data as the best-fitting model. Since [Davis et al. \(2006\)](#) proposed a specific MDL applied to change-points estimation, this criterion has been studied by many scholars and applied to various model selection problems. For example, [Davis and Yau \(2013\)](#), [Davis et al. \(2016\)](#) discuss the consistency of MDL model selection procedure, [Aue et al. \(2014\)](#) proposed a criterion based on MDL principle that could solve both variable selection and change-points estimation, [Mhalla et al. \(2020\)](#), [Woody et al. \(2021\)](#), [Shi et al. \(2022\)](#), among others, success in applying MDL criterion to a variety of practical applications.

Furthermore, it is worth mentioning that since the search space (consisting of m , τ_j , p_j and θ_j) is huge, practical optimization of this criterion is not a trivial task. [Davis et al. \(2006\)](#), [Aue et al. \(2014\)](#), [Doerr et al. \(2017\)](#), among others, have pointed out that genetic algorithm is an effective way to solve this difficulty. However, although the genetic algorithm constructed by them has the characteristics of fast search speed, strong randomness, simple process and strong flexibility, it does not take into account the precocious characteristics of genetic algorithm. Prematurity is a common problem of many global optimization algorithms, that is, the algorithm loses the population diversity prematurely, and then converges to the local optimal solution. For genetic algorithm, it is difficult to introduce new genes through selection and crossover operation, and only mutation operation can make population transfer. Thus, GA will remain in the old state for a very long time if the probability of mutation is small. Search is ineffective and precocious may eventually result. To effectively explore a better solution, a locally jittering the chromosome method, the simulated annealing process, is used to modify the classical GA ([Davis et al., 2006](#)) in this paper. The details are described in [Section 4.6](#).

The main contributions of this article are as follows. First, we propose the MCP-GINAR process to model a class of nonstationary count time series, and solve the multiple change-points estimation problem by using the MDL criterion. It includes the number of change-points, the position of change-points, the order of each segment and its parameters. Second, we discuss respectively the consistency theorems of parameters based on the two case, the number of change-points known and unknown. Third, we propose an automatic piecewise generalized integer autoregressive modeling program with simulated annealing (Auto-PGINARM-SA) to solve the optimizing problems of MDL criterion. In particular, the simulated annealing process makes up for the precocious problem of the traditional genetic algorithm.

The rest contents of this article are organized as follows. In [Section 2](#), we state some statistical properties and inferences of GINAR(p) model. In [Section 3](#), we set some notations, derive the estimation procedure and provide the consistency of parameters. [Section 4](#) describes the implementation process of Auto-PGINARM-SA procedure. In [Section 5](#), we study the performance of the Auto-PGINARM-SA via simulation, and apply the procedure to three applications in [Section 6](#). The article ends with a conclusion section and all proofs are given in [Appendix](#).

2 Statistical Inferences for GINAR(p) model

In this section, we state some statistical properties and inferences of the j -th piece GINAR(p_j) model. Considering the strict stationarity and ergodicity of the GINAR(p_j) process and the fact that GINAR(p_j) can be written as the AR(p_j) process will be helpful for us to establish the consistency of the parameter estimators. Therefore, we condense the conclusions verified by scholars into the following two Remarks.

Remark 1 *If $0 < \sum_{i=1}^{p_j} \alpha_{i,j} < 1$, then there exists a unique strictly stationary and ergodic $\{X_{t,j}\}_{t=1}^{n_j}$ that satisfies (1.4) (Zhang et al. (2010)). Additionally, if each segment is strictly stationary and ergodic GINAR process, we refer to the MCP-GINAR process (1.2) as a piecewise stationary process.*

Remark 2 *Let $\{X_{t,j}\}_{t=1}^{n_j}$ be a GINAR(p_j) process satisfying (1.4). Then $\{X_{t,j}\}_{t=1}^{n_j}$ is an AR(p_j) that can be written as*

$$e_{t,j} = \sum_{k=0}^{p_j} \alpha_{k,j} (X_{t-k,j} - \mu_{X_j}), \quad (2.1)$$

where $\alpha_{0,j} = 1$, μ_{X_j} is the mean of the j -th piece $\{X_{t,j}\}_{t=1}^{n_j}$, $e_{t,j}$ is a white noise process of variance $\sigma_{e_j}^2 = \mu_{X_j} \sum_{k=1}^{p_j} \beta_{k,j} + \sigma_{Z_j}^2$, $\beta_{k,j}$ and $\sigma_{Z_j}^2$ are the variance of the variables $B_{k,j}$ and $Z_{t,j}$ respectively (Latour (1998)).

2.1 Poisson quasi-maximum likelihood

The MDL can be regarded as the negative of the sum of the log-likelihood for each of the segments plus a penalty term which penalizes the size of the model. In this study, the Poisson quasi-maximum likelihood (PQML) is used as the cost function of MDL criterion. On the one hand, if the maximum likelihood (ML) proposed by Bu et al. (2008) is used as the cost function, since the transition probabilities in ML are written using the convolution formula, the form is too complex, it is challenging to confirm the corresponding conditions when discussing the consistency of the number of change-points and the location of change-points. On the other hand, as mentioned in Ahmad and Francq (2016), it is known that certain ML can be consistent and asymptotically normal for the parameters of the conditional mean and variance, even if the actual conditional distribution is not the one which is assumed by the ML. Noting that the parameters in GINAR(p) can be treated as mean parameters and that PQML can be shown to have consistency and asymptotic normality under certain assumptions, so the PQML is a great option as the cost function.

Given all the past observations, the conditional Poisson quasi-maximum log-likelihood of the j -th piece, $\mathbf{x}_j = \{X_{t,j}\}_{t=-p}^{n_j}$, is obtained by

$$L_{n_j}^{(j)}(\boldsymbol{\theta}_j; p_j, \mathbf{x}_j) = \sum_{t=1}^{n_j} [X_{t,j} \log \xi_{t,j}(\boldsymbol{\theta}_j; p_j | X_{s,j}, s < t) - \xi_{t,j}(\boldsymbol{\theta}_j; p_j | X_{s,j}, s < t)] \quad (2.2)$$

$$= \sum_{t=1}^{n_j} \ell_t^{(j)}(\boldsymbol{\theta}_j; p_j, X_{t,j} | X_{s,j}, s < t),$$

where $\xi_{t,j}(\boldsymbol{\theta}_j; p_j | X_{s,j}, s < t) = \sum_{k=1}^{p_j} \alpha_{k,j} X_{t-k,j} + \gamma_j$. It is important to note that $\mathbf{x}_0 = \{X_{t,1}\}_{t=-p}^{-1}$ for the first piece, where \mathbf{x}_0 is a set of initial integer values. Then the PQML estimator of $\boldsymbol{\theta}_j$ is defined by

$$\hat{\boldsymbol{\theta}}_j = \arg \max_{\boldsymbol{\theta}_j \in \Theta_j(p_j)} L_{n_j}^{(j)}(\boldsymbol{\theta}_j; p_j, \mathbf{x}_j).$$

Assuming that $0 < \sum_{i=1}^{p_j} \alpha_{p_i} < 1$ and $E(X_{1,j}) < \infty$, as stated in Section 3.7. of [Ahmad and Francq \(2016\)](#), $\hat{\boldsymbol{\theta}}_j$ satisfy the following asymptotic normality

$$\sqrt{n_j}(\hat{\boldsymbol{\theta}}_j - \boldsymbol{\theta}_j^0) \xrightarrow{d} N(0, \boldsymbol{\Sigma}_j) \quad \text{as } n_j \rightarrow \infty,$$

where $\boldsymbol{\theta}_j^0$ denote the true parameter value of $\boldsymbol{\theta}_j$. To simplify notation, denote $\xi_{t,j}(\boldsymbol{\theta}_j) = \xi_{t,j}(\boldsymbol{\theta}_j; p_j | X_{s,j}, s < t)$, then the asymptotic variance matrix of the j -th piece PQML estimator can be consistently estimated by $\boldsymbol{\Sigma}_j = \mathbf{J}_j^{-1} \mathbf{I}_j \mathbf{J}_j^{-1}$ with

$$\mathbf{J}_j = \frac{1}{n_j} \sum_{t=1}^{n_j} \frac{1}{\xi_{t,j}(\boldsymbol{\theta}_j)} \frac{\partial \xi_{t,j}(\boldsymbol{\theta}_j)}{\partial \boldsymbol{\theta}_j} \frac{\partial \xi_{t,j}(\boldsymbol{\theta}_j)}{\partial \boldsymbol{\theta}_j^T} \Bigg|_{\boldsymbol{\theta}_j = \hat{\boldsymbol{\theta}}_j}, \quad (2.3)$$

$$\mathbf{I}_j = \frac{1}{n_j} \sum_{t=1}^{n_j} \left(\frac{X_{t,j}}{\xi_{t,j}(\boldsymbol{\theta}_j)} - 1 \right)^2 \frac{\partial \xi_{t,j}(\boldsymbol{\theta}_j)}{\partial \boldsymbol{\theta}_j} \frac{\partial \xi_{t,j}(\boldsymbol{\theta}_j)}{\partial \boldsymbol{\theta}_j^T} \Bigg|_{\boldsymbol{\theta}_j = \hat{\boldsymbol{\theta}}_j}. \quad (2.4)$$

3 Main result

In this section, we first introduce the MDL criterion for this MCP-GINAR model based on PQML. And then we present the main results of the paper. Theorem 1 shows the strong consistency of the MDL procedure when the number of change-points is known. Theorem 2 not only shows the weak consistency of the MDL procedure when the number of change-points is unknown, but also gives the rate of convergence of the change-points estimators. Furthermore, Theorems 3 gives the strongly consistency analog of Theorems 2, where stronger moment conditions are required.

For the sake of readability, we provide the following notations and assumption, and their corresponding explanations before introducing the MDL criterion.

Notations:

- Denote this whole class of MCP-GINAR models by \mathcal{M} and any model from this class by $\mathcal{F} \in \mathcal{M}$.
- Let $\boldsymbol{\lambda} = (\lambda_1, \dots, \lambda_m)$, $0 < \lambda_1 < \dots < \lambda_m < 1$, satisfy $\tau_j = [\lambda_j n]$, where $[x]$ is the greatest integer that is less than or equal to x .

- Upper bounds for GINAR orders p are represented by P_0 . Setting $\mathbf{p} = (p_1, \dots, p_{m+1})$ belongs to the parameter domain $\mathcal{P} = (0, P_0]^{m+1} \cap \mathbb{Z}^{m+1}$, $\boldsymbol{\theta} = (\boldsymbol{\theta}_1, \dots, \boldsymbol{\theta}_{m+1})$ belongs to the parameter domain $\Theta = \prod_{j=1}^{m+1} \Theta_j(p_j)$.
- If the number and location of change points are known, the conditional Poisson quasi-maximum log-likelihood of the j -th piece can be given by (2.2). However, in practice, both the number of change-points and the locations of the change-points are unknown. As a result, for any observation $x_{i,j}$, its “observed past”, is in fact

$$(\mathbf{x}_0, x_{1,1}, \dots, x_{n_1,1}, \dots, x_{1,j}, \dots, x_{i-1,j}),$$

or equivalently, $\tilde{\mathbf{x}}_{i,j} \equiv (\mathbf{x}_0, x_1, x_2, \dots, x_{\tau_{j-1}+i-1})$, where $\mathbf{x}_0 = \{X_{t,1}\}_{t=-p}^{-1}$ is the initial value vector. The conditional Poisson quasi log-likelihood of the j -th piece is then given by

$$\begin{aligned} \tilde{L}_{n_j}^{(j)}(\boldsymbol{\theta}_j; p_j, \mathbf{x}_j) &= \sum_{t=1}^{n_j} x_{t,j} \log \xi_{t,j}(\boldsymbol{\theta}_j; p_j | \tilde{\mathbf{x}}_{i,j}) - \xi_{t,j}(\boldsymbol{\theta}_j; p_j | \tilde{\mathbf{x}}_{i,j}) \\ &= \sum_{t=1}^{n_j} \ell_t^{(j)}(\boldsymbol{\theta}_j; p_j, \tilde{\mathbf{x}}_{i,j}). \end{aligned} \quad (3.1)$$

Assumptions:

- To ensure the piecewise stationary, for each segment, assume that $\boldsymbol{\theta}_j$ is an interior point of the compact space $\Theta_j(p_j)$ and satisfies $\sum_{i=1}^{p_j} \alpha_{i,j} < 1$, $\alpha_i \geq 0$ for $i = 1, \dots, p_j$.
- To accurately estimate the specified GINAR parameter values, the segments must have a sufficient number of observations. If not, the estimation is overdetermined and the likelihood has an infinite value. So to ensure identifiability of the change-points, when we search for the change-points, we assume that there exists a $\epsilon_\lambda > 0$ such that $\epsilon_\lambda < \min_{1 \leq j \leq m} (|\lambda_j - \lambda_{j-1}|)$ and set

$$A_{\epsilon_\lambda}^m = \{\boldsymbol{\lambda} \in (0, 1)^m, 0 < \lambda_1 < \dots < \lambda_m < 1, \lambda_j - \lambda_{j-1} \geq \epsilon_\lambda, j = 1, \dots, m\}.$$

So under this restriction the number of change points is bounded by $M_0 = \lceil 1/\epsilon_\lambda \rceil + 1$.

Let the vector $(m, \boldsymbol{\lambda}, \mathbf{p}, \boldsymbol{\theta})$ specifies completely a model of a non-stationary time series $\{X_t\}_{t=1}^n$ defined in (1.2). According to Davis and Yau (2013), the MDL for this model is given by

$$\begin{aligned} \text{MDL}(m, \boldsymbol{\lambda}, \mathbf{p}, \boldsymbol{\theta}) &= \log(m) + (m+1) \log n + \sum_{j=1}^{m+1} \log(p_j) + \sum_{j=1}^{m+1} \frac{p_j + 1}{2} \log(n_j) \\ &\quad - \sum_{j=1}^{m+1} \tilde{L}_{n_j}^{(j)}(\boldsymbol{\theta}_j; p_j, \mathbf{x}_j). \end{aligned}$$

The estimators of the number of change-points, the locations of change-points and the parameters in each of the segments are given by the vector $(\hat{m}_n, \hat{\boldsymbol{\lambda}}_n, \hat{\boldsymbol{p}}_n, \hat{\boldsymbol{\theta}}_n)$, that is

$$(\hat{m}_n, \hat{\boldsymbol{\lambda}}_n, \hat{\boldsymbol{p}}_n, \hat{\boldsymbol{\theta}}_n) = \arg \min_{\substack{m \leq M_0, \boldsymbol{\lambda} \in A_{\epsilon_\lambda}^m, \\ \boldsymbol{p} \in \mathcal{P}, \boldsymbol{\theta} \in \Theta}} \text{MDL}(m, \boldsymbol{\lambda}, \boldsymbol{p}, \boldsymbol{\theta}), \quad (3.2)$$

where $\hat{\boldsymbol{\lambda}}_n = (\hat{\lambda}_1, \dots, \hat{\lambda}_{\hat{m}_n})$, $\hat{\boldsymbol{p}}_n = (\hat{p}_1, \dots, \hat{p}_{\hat{m}_n+1})$, $\hat{\boldsymbol{\theta}}_n = (\hat{\boldsymbol{\theta}}_1, \dots, \hat{\boldsymbol{\theta}}_j, \dots, \hat{\boldsymbol{\theta}}_{\hat{m}_n+1})$, with

$$\hat{\boldsymbol{\theta}}_j = \arg \max_{\boldsymbol{\theta}_j \in \Theta_j(\hat{p}_j)} \tilde{L}_{n_j}^{(j)}(\boldsymbol{\theta}_j; \hat{p}_j, \hat{\boldsymbol{x}}_j),$$

and $\hat{\boldsymbol{x}}_j = \{x_t\}_{t=[n\hat{\lambda}_{j-1}]+1}^{t=[n\hat{\lambda}_j]}$.

Let $\{x_t\}_{t=1}^n$ be observations from a piecewise stationary process (1.2) specified by the true value vector $(m^0, \boldsymbol{\lambda}^0, \boldsymbol{p}^0, \boldsymbol{\theta}^0)$, where $\boldsymbol{\lambda}^0 = (\lambda_1^0, \dots, \lambda_{m^0}^0)$, $\boldsymbol{p}^0 = (p_1^0, \dots, p_{m^0}^0)$, $\boldsymbol{\theta}^0 = (\boldsymbol{\theta}_1^0, \dots, \boldsymbol{\theta}_{m^0}^0)$. We first give the following Theorem 1, which indicates the assumption and the result about the convergence of the change-points locations and the order parameter estimators when the number of change-points is known.

Theorem 1 *Assume that $E|X_{t,j}|^{2+\eta} < \infty$ for some $\eta > 0$. Suppose the number of change-points m^0 is known and we estimate the locations and the model parameter by*

$$(\hat{\boldsymbol{\lambda}}_n, \hat{\boldsymbol{p}}_n, \hat{\boldsymbol{\theta}}_n) = \arg \min_{\substack{\boldsymbol{\lambda} \in A_{\epsilon_\lambda}^{m^0}, \\ \boldsymbol{p} \in \mathcal{P}, \boldsymbol{\theta} \in \Theta}} \text{MDL}(m^0, \boldsymbol{\lambda}, \boldsymbol{p}, \boldsymbol{\theta}). \quad (3.3)$$

Then, $\hat{\boldsymbol{\lambda}}_n \xrightarrow{a.s.} \boldsymbol{\lambda}^0$ and for each segment the estimated model does not underestimate the true model.

The following two theorems will discuss consistent results under the condition of the number of change-points is unknown.

Theorem 2 (Weak Consistency) *Assume that $E(X_{t,j})^{4+\eta} < \infty$. The estimator $(\hat{m}_n, \hat{\boldsymbol{\lambda}}_n, \hat{\boldsymbol{p}}_n, \hat{\boldsymbol{\theta}}_n)$ is defined in (3.2). Then we have weak consistency of MDL model selection, i.e.,*

$$\hat{m}_n \xrightarrow{P} m^0, \quad \hat{\boldsymbol{\lambda}}_n \xrightarrow{P} \boldsymbol{\lambda}^0, \quad \hat{\boldsymbol{p}}_n \xrightarrow{P} \boldsymbol{p}^0, \quad \hat{\boldsymbol{\theta}}_n \xrightarrow{P} \boldsymbol{\theta}^0,$$

and for each λ_j^0 , $j = 1, \dots, m^0$, there exists a $\hat{\lambda}_{j'} \in \hat{\boldsymbol{\lambda}}_n$, $1 \leq j' \leq \hat{m}_n$, such that for any $\kappa > 0$,

$$\left| \hat{\lambda}_{j'} - \lambda_j^0 \right| = O_p(n^{\kappa-1}).$$

After strengthening the moment condition, the following theorem shows strong consistency in the MDL model selection process.

Theorem 3 (Strong Consistency) *Assume that $E(X_{t,j})^{8+\eta} < \infty$. The estimator $(\hat{m}_n, \hat{\boldsymbol{\lambda}}_n, \hat{\boldsymbol{p}}_n, \hat{\boldsymbol{\theta}}_n)$ is defined in (3.2). Then we have strong consistency of MDL model selection, i.e.,*

$$\hat{m}_n \xrightarrow{a.s.} m^0, \quad \hat{\boldsymbol{\lambda}}_n \xrightarrow{a.s.} \boldsymbol{\lambda}^0, \quad \hat{\boldsymbol{p}}_n \xrightarrow{a.s.} \boldsymbol{p}^0, \quad \hat{\boldsymbol{\theta}}_n \xrightarrow{a.s.} \boldsymbol{\theta}^0,$$

and for each λ_j^0 , $j = 1, \dots, m^0$, there exists a $\hat{\lambda}_{j'} \in \hat{\boldsymbol{\lambda}}_n$, $1 \leq j' \leq \hat{m}_n$, such that

$$\left| \hat{\lambda}_{j'} - \lambda_j^0 \right| = o(n^{-\frac{1}{2}}), \quad \text{a.s.},$$

furthermore, if the order $p_{j'}^0$ of the j' -th piece true model is specified, then

$$\hat{\boldsymbol{\theta}}_{j'}(\hat{\lambda}_{j'-1}, \hat{\lambda}_{j'}) - \boldsymbol{\theta}_j^0 = O_p\left(\sqrt{\frac{\log \log n}{n}}\right),$$

where

$$\begin{aligned} \hat{\boldsymbol{\theta}}_{j'}(\hat{\lambda}_{j'-1}, \hat{\lambda}_{j'}) &= \arg \max_{\boldsymbol{\theta}_{j'} \in \Theta_{j'}(p_{j'}^0)} \tilde{L}_{n_{j'}}^{(j')}(\boldsymbol{\theta}_{j'}, \hat{\lambda}_{j'-1}, \hat{\lambda}_{j'}; p_{j'}^0, \hat{\boldsymbol{x}}_{j'}) \\ &= \arg \max_{\boldsymbol{\theta}_{j'} \in \Theta_{j'}(p_{j'}^0)} \left(\sum_{t=[\hat{n}_{j'} \hat{\lambda}_{j'-1}]+1}^{[\hat{n}_{j'} \hat{\lambda}_{j'}]} \ell_t^{(j')}(\boldsymbol{\theta}_{j'}; p_{j'}^0, |x_{s,j'}, s < t) \right). \end{aligned}$$

Remark 3 Clearly, from the results obtained in Theorem 2 and Theorem 3, the convergence rate of the PQML estimator $\hat{\boldsymbol{\theta}}$ is not affected even when the estimated piece may not be fully inside a stationary piece of a time series but involves part of the adjacent stationary pieces.

4 Genetic Algorithm

Genetic Algorithm (GA), a global search optimization technique, was first proposed by Holland and is based on the principle of natural selection. Holland described this concept in his book, "Adaptation in Natural and Artificial Systems". GA is a population-based search algorithm that applies the survival of the fittest concept. By applying genetic operators repeatedly to people already existing in the population, new populations are created. The main components of GA are chromosome representation, selection, crossover, mutation, and fitness function computation.

As the era of data arrived, many academics quickly investigated and invented numerous algorithms. The GA package or function is now available in several software, including the SBRect package for the statistical language R (Doerr et al. (2017)) and the ga function for MATLAB. However, defining special chromosome coding, crossover, and mutation, as well as adding specific optimization processes (such as annealing processes), often helps to improve the accuracy and speed of optimization results, especially for the optimising problems being studied.

In Davis et al. (2006), a very classical and comprehensive genetic algorithm automatic piecewise autoregressive modelling process (Auto-PARM) was suggested for the optimal MDL criterion. In the article that followed, published in Aue et al. (2014), the algorithm was still applied for data segmentation and variable selection based on quantile regression. In recent years numerous scholars have addressed their experiences with genetic algorithms. In light of these experiences, we enhanced Auto-PARM in two aspects: modifying the **crossing**

operation and adding the **annealing process**, which we dubbed automatic piecewise generalized integer autoregressive modeling program with simulated annealing (Auto-PGINARM-SA). Although some of the steps are the same as those of [Davis et al. \(2006\)](#), we need to repeat them to ensure the integrity of the algorithm for the sake of readability.

4.1 Chromosome representation

The representation of a potential solution as a chromosome affects a GA’s performance, and for the current issue (minimizing (3.2)), a chromosome should contain all the information that any $\mathcal{F} \in \mathcal{M}$ could possibly need regarding the change-points, τ_j , and the j -th segment GINAR orders, p_j . Poisson quasi-maximum likelihood estimators of other model parameters can be uniquely calculated once these quantities have been established. Here we use the same chromosome representation as in [Davis et al. \(2006\)](#), a chromosome $\delta = (\delta_1, \dots, \delta_n)$ is of length n with gene values δ_t defined as

$$\delta_t = \begin{cases} p_j & \text{if } t = \tau_{j-1} \text{ and the GINAR order for the } j\text{-th piece is } p_j, \\ -1 & \text{if no change-point at } t. \end{cases}$$

In practice, the following constraints are imposed on each δ . First, an upper bound P_0 is put on the order p_j of the GINAR process in the algorithm’s actual implementation. Given that we require a large P_0 to capture complicated sequences and that P_0 cannot exceed the number of observations n for simple sequences, there doesn’t appear to be a single value for P_0 . In keeping with past published experience, we decided to set $P_0 = 20$ in our simulation. At the same time, the following “minimum span” restriction is imposed to δ in order to have sufficient observed data for parameter estimation. A piece of \mathcal{F} must have at least m_p observations if the GINAR order of the piece is p . To guarantee that there are enough observations to produce estimators of the GINAR(p) process parameters, this preset integer m_p was used. Table 1 contains the relevant minimum span m_p .

Table 1: Values of m_p for order p .

p	0–1	2	3	4	5	6	7–10	11–20
m_p	10	12	14	16	18	20	25	50

4.2 Initial Population Generation

For the chromosome $\delta = (\delta_1, \dots, \delta_n)$, δ_t will be a change-point with probability $\pi_B = 10/n$ and -1 with probability $1 - \pi_B$. Once δ_t is declared to be a break, select a value for p_t from $\{0, \dots, P_0\}$ with equal probabilities and set $\delta_t = p_t$. Then to ensure the minimum span constraint, set the next $m_{p_t} - 1$ genes δ_i (i.e., $\delta_{t+1}, \dots, \delta_{t+m_{p_t}-1}$) is -1 . For the next gene $\delta_{t+m_{p_t}}$ we repeat the process of δ_t until the last gene δ_n . Just to be clear, for the first gene, δ_1 , must serve as the beginning point of the first piecewise, thus we choose directly from the uniform distribution with values $\{0, \dots, P_0\}$ and set $\delta_1 = p_1$.

4.3 Selection

Once the first generation of random chromosomes is generated, we select some of the chromosomes with good genes as parents for the following crossover and mutation operations. The probability of the two parents is inversely proportional to their ranking in order of MDL values. In other words, chromosomes with lower MDL values are more likely to be selected. As for the select method, in our simulation, we chose the roulette to select the parents.

After parental selection, crossover and mutation operations are applied to produce offspring, which will form a second generation. Offspring tend to be better than their parents because they are better solutions to optimizing problems. The probability of carrying out a crossover operation in this implementation is set to π_C , while the probability of carrying out a mutation operation is set to $1 - \pi_C$, where $\pi_C = (n - 10)/n$. Next, the crossover and mutation operations used in this paper are introduced respectively.

4.4 Crossover

We first introduce the following two crossover operations.

Uniform crossover: this operation on two parent strings $\delta_f = (\delta_1^{(1)}, \dots, \delta_n^{(1)})$ and $\delta_m = (\delta_1^{(2)}, \dots, \delta_n^{(2)})$ is defined as follows. The offspring string $\delta_c = (\delta_1^{(3)}, \dots, \delta_n^{(3)})$ is constructed by independently choosing the string entries from the two parents with equal probabilities, i.e.,

$$\delta_t^{(3)} = \begin{cases} \delta_t^{(1)} & \text{with probability } 1/2; \\ \delta_t^{(2)} & \text{with probability } 1/2. \end{cases}$$

Pertaining to the Uniform crossover, for $t = 1$, $\delta_1^{(3)}$ takes on the corresponding value $\delta_1^{(3)} = p_1$ from either the first parent $\delta_1^{(1)}$ or second parent $\delta_1^{(2)}$ with equal probabilities, the next $m_{p_1} - 1$ genes are set to -1 . Then for $t = m_{p_1} + 1$, $\delta_{m_{p_1}+1}^{(3)}$ is again taken from the first or second parent with equal probability. If this value is -1 , then the same gene-inheriting process is repeated for the next gene in line (i.e., $\delta_{m_{p_1}+2}^{(3)}$). If this value is not -1 , then it is a nonnegative integer p_j denoting the GINAR order of the current piece. In this case the minimum span constraint is imposed (i.e., the next $m_{p_j} - 1$ are set to -1), and repeat the same genetic process until δ_n .

One-point crossover: this operation on two parent strings $\delta_f = (\delta_1^{(1)}, \dots, \delta_n^{(1)})$ and $\delta_m = (\delta_1^{(2)}, \dots, \delta_n^{(2)})$, an index k is chosen uniformly at random from $1, \dots, n$. The child δ_c consist of the first k values from δ_f and the last $n - k$ values from δ_m , i.e

$$\delta_c = (\delta_1^{(1)}, \dots, \delta_k^{(1)}, \delta_{k+1}^{(2)}, \dots, \delta_n^{(2)}).$$

Due to the minimum span constraint, the number of $m_{p_t} - 1$ following the change point $\delta_t^{(1)}$ with order p_t should be omitted during the random selection of k , which means that k cannot be picked in $\delta_{t+1}^{(1)}, \dots, \delta_{t+m_{p_t}-1}^{(1)}$.

Currently, the majority of genetic algorithms only employ one sort of crossover, such as uniform crossover, which is adopted by [Davis et al. \(2006\)](#) and [Aue et al. \(2014\)](#). However, according to the discussion in [Doerr et al. \(2017\)](#), uniform crossover significantly raises fitness

and one-point crossover supports the building block structure of the underlying problem. Strings generated by mutation and uniform crossover look empirically good, but often have “a flaw in one or two places”. In contrast, one-point crossover make it possible to integrate the flaw-less parts of two strings to an almost perfect one. We will apply the two types of crossover operations mentioned above in this study and draw on the knowledge of other researchers who have studied this approach. Although it is evident from the analysis above that using two different types of crossover is absolutely necessary, we nevertheless believe subjectively that uniform crossover is more secure, hence the uniform crossover is primarily employed in the two techniques. For the two crossover operations, we assume that if the crossing occurs, the probability of a uniform crossing is

$$P(\text{uniform crossover occur}) = 1 - P(\text{one-point crossover occur}) = \pi_{cross} = 0.7.$$

4.5 Mutation

One child is produced from one parent in the case of mutation. This method avoids the issue of too quickly convergent to a suboptimal solution by giving the child chromosome more opportunity to explore the search space. This process starts with the second change-point t , and every δ_t (subject to the minimum span constraint) can take one of the following three possible values: It does three things: (a) with probability π_P , it takes the parent’s corresponding δ_t value; (b) with probability π_N , it takes the value -1 ; and (c) with probability $1 - \pi_P - \pi_N$, it takes a fresh GINAR order (p_j) that was produced at random. In the present implementation, π_P and π_N are both set to 0.3. It should be noted that for $t = 1$, only (a) and (c) mutations are carried out, and that $\pi_P = 0.5$ and $\pi_N = 0$.

4.6 Simulated Annealing

The concept of annealing was first proposed by [Kirkpatrick et al. \(1983\)](#) and developed by Metropolis, and it has proven to be a successful method to address the issue of precocious. Its main idea is to randomly select a solution in the neighborhood of the optimal solution δ , and then compare them to determine which is best. Taking into account the parameters to be optimized, we introduce the following two annealing operations.

Annealing of the location of change-points τ . This operation on an optimal chromosome of the current generation $\delta = (\delta_1, \dots, \delta_n)$ performs the following operation to randomly select a solution δ_{A_τ} in its neighborhood. If t is a change-point with order p_t , randomly select an integer s from a range $[a, b]$, makes $\delta_{t+s} = \delta_t = p_t$, and then $\delta_t = -1$. In the present implementation, $a = -10, b = 10$. Of course, if the minimum span constraint cannot be guaranteed after such changes, the operation on δ_t is abandoned, and the operation on the next change point is repeated until the last change point. And then we’re going to get a neighborhood solution δ_{A_τ} .

Annealing of order p . In this operation, for the j -th piece, which contains data $\mathbf{x}_t = (x_{j_1}, \dots, x_{j_s})$, corresponding to the gene segment in the chromosome $(\delta_{j_1}, \dots, \delta_{j_s})$. Through the Yule-Walker parameter estimation expression in [Silva and Silva \(2006\)](#), the estimator

$(\hat{\alpha}_{j_1}, \dots, \hat{\alpha}_{j_{P_0}})$ can be calculated based on \mathbf{x}_t . Then make the following substitution for the change-point location gene, $\delta_{t_1} = \max_u \{\hat{\alpha}_{j_u} > \pi_{A_p}, u = 1, 2, \dots, P_0\}$ (here we set $\pi_{A_p} = 0.05$). The process is also abandoned if the minimum span constraint cannot be guaranteed following such a change and the subsequent part is repeated until the last piece. And then we're going to get a neighborhood solution δ_{A_p} .

In conclusion, perform the following steps for the annealing process. A new population is produced once the crossover and mutation are finished. In this population, the chromosome δ_1 with the lowest MDL value was found. Then, apply the two annealing operations mentioned above to δ_1 to obtain its two neighborhood solutions, δ_{A_τ} and δ_{A_p} . Make $\delta'_1 = \arg \min_{\delta \in \{\delta_1, \delta_{A_\tau}, \delta_{A_p}\}} \text{MDL}(\delta)$, and let $\delta_1 = \delta'_1$ be the final step.

4.7 Elitist step and Island model

Two more phases, the elitist step and the island model, are carried out to hasten the convergence to an optimal solution. In the elitist stage, The best chromosome from the present generation will take the place of the worst chromosome from the next generation. This ensures the monotonicity of the search process and conserves the best chromosome in each generation. The island model is carried out using parallel implementations, and NI (number of islands) GAs are run simultaneously in NI different subpopulations. After every J generations, the best H chromosomes from the $(j - 1)$ th island will replace the worst H chromosomes from the j th island, $j = 2, \dots, NI$ (for $j = 1$ the worst H chromosomes are replaced by the best chromosomes from the NI -th island). Here, $NI = 40, J = 5, H = 2$, and a subpopulation size of 40 are used in the implementation.

5 Simulation

To evaluate the finite-sample performance of the proposed Auto-PGINARM-SA procedure, we conduct extensive simulation studies and split the simulation studies into the following three parts. First, Auto-PGINARM-SA was compared with Auto-PARM, proposed by [Davis et al. \(2006\)](#). Note that Auto-PARM is for autoregressive process, while the problem we studied is general integer-valued autoregressive process, so we replace the Gaussian quasi likelihood function in Auto-PARM with the PQML function and name it Auto-PGINARM procedure. In the second simulation, MDL was contrasted with the existing method penQLIK ([Diop and Kengne \(2021b\)](#)). In the last part, Six sets of simulation are utilised to study the consistency conclusion. For convenience, we first introduce the following two INAR(p) processes that are primarily used in simulations.

The j -th piece process $\{X_{t,j}\}$ is said to INAR(p_j) process based on the binomial thinning operator (BiINAR(p_j)) if it is determined by the recursion:

$$X_{t,j} = \alpha_{1,j} \circ X_{t-1,j} + \dots + \alpha_{p_j,j} \circ X_{t-p_j,j} + Z_{t,j}, \quad (5.1)$$

where “ \circ ” is the binomial thinning operator, which is proposed by [Steutel and Van Harn \(1979\)](#) and defined as: $\alpha \circ X = \sum_{i=1}^X B_i(\alpha)$, the counting series $\{B_i(\alpha)\}$ is an independent and

identically distributed (i.i.d.) Bernoulli random sequence with mean α , $\{Z_{t,j}\}$ is a sequence of i.i.d. Poisson random variables with mean γ .

The j -th piece process $\{X_{t,j}\}$ is said to INAR(p_j) process based on the negative binomial thinning operator (NBINAR(p_j)) if it is determined by the recursion:

$$X_{t,j} = \alpha_{1,j} * X_{t-1,j} + \dots + \alpha_{p_j,j} * X_{t-p_j,j} + Z_{t,j}, \quad (5.2)$$

where “ $*$ ” is the negative binomial thinning operator of [Ristić et al. \(2009\)](#), it is defined as $\alpha * X = \sum_{i=1}^X W_i(\alpha)$, the counting series $\{W_i(\alpha)\}$ is a sequence of i.i.d. geometric random variables with parameter $\alpha/(1+\alpha)$, $\{Z_{t,j}\}$ is a sequence of i.i.d. Geometric random variables with parameter $\gamma/(1+\gamma)$.

All simulations are carried out using the MATLAB software. The empirical results displayed in the tables, including the true positive rate (TPR) that is the proportion of informative points are correctly identified, the empirical biases (Bias) and mean square errors (MSE), are computed over 1000 replications.

5.1 Efficiency of Simulated Annealing

The objective of the following scenario MCP-BiINAR is to evaluate the performance of simulated annealing by comparing the optimization efficacy of Auto-PGINARM and Auto-PGINARM-SA.

$$X_t = \begin{cases} 0.5 \circ X_{t-1,1} + Z_{t,1}, & 1 \leq t \leq 400, \\ 0.2493 \circ X_{t-1,2} + 0.254 \circ X_{t-2,2} + 0.2967 \circ X_{t-3,2} + Z_{t,2}, & 401 \leq t \leq 800, \\ 0.4 \circ X_{t-1,3} + Z_{t,3}, & 801 \leq t \leq 1000, \end{cases}$$

where “ \circ ” is defined in [\(5.1\)](#) and $\{Z_{t,j}\}_{j=1,2,3}$ is a sequence of i.i.d. Poisson random variables with mean γ_j , and $(\gamma_1, \gamma_2, \gamma_3) = (0.5, 1, 0.5)$.

Table 2 provides a summary of all the findings, including the TPR of the number of change points (TPR(m)) and the order p of each segment (TPR(p)), the Bias and MSE of the change-points locations, the average MDL value ($\overline{\text{MDL}}$), average time(s), annealing frequency, and the relative frequency when the MDL value of Auto-PGINARM-SA was smaller in 1000 replications. The following results can be seen from the Table 2. Out of 1000 replications, annealing ran 89912 times, demonstrating its effectiveness in Auto-PGINARM-SA. The results of Bias, MSE, and TPR(p) demonstrate that Auto-PGINARM-SA is essentially always superior to Auto-PGINARM. Simulated annealing significantly improves the accuracy of MDL optimization, particularly for the estimation of p_3 in the third segment. It is not difficult to see from the average time that the simulated anneal process improves the speed of finding the optimal solution. In terms of MDL value, the average MDL value calculated by Auto-PGINARM-SA is smaller. Remarkably, Auto-PGINARM-SA was able to find a better solution 982 times out of 1000 replications. All conclusions indicate that, with the assistance of simulated annealing, Auto-PGINARM-SA could quickly find better solutions and effectively solve the precocious problem.

Table 2: Summary of the performance of simulated annealing by comparing the results of Auto-PGINARM and Auto-PGINARM-SA under the scenario MCP-BiINAR.

	Auto-PGINARM					Auto-PGINARM-SA				
	Bias	MSE	TPR(p)	TPR(m)	$\overline{\text{MDL}}$	Bias	MSE	TPR(p)	TPR(m)	$\overline{\text{MDL}}$
p_1	0.0000	0.0000	1	0.99	-713.5010	0.0000	0.0000	1	0.989	-716.6701
p_2	-0.0020	0.0040	0.996			0.0000	0.0020	0.998		
p_3	0.1960	0.2404	0.798			0.0060	0.0320	0.974		
λ_1	-0.0013	0.0001				-0.0003	0.0001			
λ_2	-0.0007	0.0000				-0.0011	0.0000			
Average time(s): 2595.251						Average time(s): 2171.780				
Annealing frequency										89812
the relative frequency of MDL(Auto-PGINARM-SA)<MDL(Auto-PGINARM)										0.982

5.2 Comparison between the MDL and penQLIK

Next, under the following scenario MCP-NBINAR, we make a comparison of MDL with the penalized contrast QLIK (penQLIK) (Diop and Kengne (2021b)) which is carried out a data-driven method, based on the slope heuristic procedure (see Baudry et al. (2012)) to calibrate the penalty term. The dynamic programming algorithm is used to minimize the penQLIK criteria.

$$X_t = \begin{cases} 0.5 * X_{t-1,1} + Z_{t,1}, & 1 \leq t \leq 300, \\ 0.4524 * X_{t-1,2} + 0.1818 * X_{t-2,2} + 0.1658 * X_{t-3,2} + Z_{t,2}, & 301 \leq t \leq 500, \\ 0.4 * X_{t-1,3} + Z_{t,3}, & 501 \leq t \leq 800, \\ 0.0252 * X_{t-1,4} + 0.1502 * X_{t-2,4} + 0.4692 * X_{t-3,4} + 0.1554 * X_{t-4,4} + Z_{t,4} & 801 \leq t \leq 1000, \end{cases}$$

where “*” is the negative binomial thinning operator, defined in (5.2), and $\{Z_{t,j}\}_{j=1,2,3,4}$ is a sequence of i.i.d. Geometric random variables with mean γ_j , respectively, and $(\gamma_1, \gamma_2, \gamma_3, \gamma_4) = (0.5, 1, 0.5, 2)$.

Considering that the order p is not taken into account in the information criterion of penQLIK, and a specific p value cannot be set in the scenario MCP-NBINAR, we respectively simulated the effect of penQLIK in the three cases of $p = 1, 2, 6$. They are denoted as penQLIK(1), penQLIK(2), penQLIK(6). In this section we not only calculate the TPR of the number of change-points, the Bias and MSE of the location of change-points, but also calculate the distance between the estimated set $\hat{\lambda}_n$ and the true change-point set λ^0 (Boysen et al. (2009)),

$$\zeta(\hat{\lambda}_n | \lambda^0) = \sup_{b \in \lambda^0} \inf_{a \in \hat{\lambda}_n} |a - b|, \quad \zeta(\lambda^0 | \hat{\lambda}_n) = \sup_{b \in \hat{\lambda}_n} \inf_{a \in \lambda^0} |a - b|.$$

which quantify the over-segmentation error and the under-segmentation error, respectively. A desirable estimator should be able to balance both quantities. All results are summarized in Table 3. To make things more intuitive, we also present the boxplot (Figure 1), which is

obtained from the bias of m , the average values of $\zeta(\hat{\lambda}_n|\lambda^0)$, $\zeta(\lambda^0|\hat{\lambda}_n)$ simulation results for the scenario MCP-NBINAR.

Clearly, different values of p have great influence on the performance of penQLIK. As can be seen from the results in the Table 3 and boxplot, although the effect of penQLIK is significantly improved when p value is relatively large, there is still a big gap between the effect of penQLIK and MDL. More intuitively, from boxplot, the $\zeta(\hat{\lambda}_n|\lambda^0)$ and $\zeta(\lambda^0|\hat{\lambda}_n)$ of penQLIK(1) and penQLIK(2) are out of balance, that is, serious under-segmentation error will occur in these two information criterion. Although penQLIK(6) obviously reduces the occurrence of the under-segmentation error, the performance is not as good as that of MDL.

Table 3: Comparison results of MDL and penQLIK under the scenario MCP-NBINAR.

Criteria	TPR(m)	$\zeta(\hat{\lambda}_n \lambda^0)$	$\zeta(\lambda^0 \hat{\lambda}_n)$	$\hat{\lambda}_n$			\hat{p}_n				
				$\hat{\lambda}_1$	$\hat{\lambda}_2$	$\hat{\lambda}_3$	\hat{p}_1	\hat{p}_2	\hat{p}_3	\hat{p}_4	
MDL	0.949	0.0210	0.0132	Bias	0.0020	-0.0020	0.0004	0.0200	-0.5290	0.0948	-0.5100
				MSE	0.0002	0.0001	0.0000	0.0242	0.6512	0.0991	0.5227
penQLIK(1)	0.206	0.0185	0.0946	Bias	0.0089	0.0012	0.0062				
				MSE	0.0015	0.0014	0.0002				
penQLIK(2)	0.296	0.0153	0.0816	Bias	0.0058	0.0022	0.0046				
				MSE	0.0006	0.0010	0.0001				
penQLIK(6)	0.613	0.0285	0.0482	Bias	0.0013	0.0031	0.0006				
				MSE	0.0010	0.0010	0.0001				

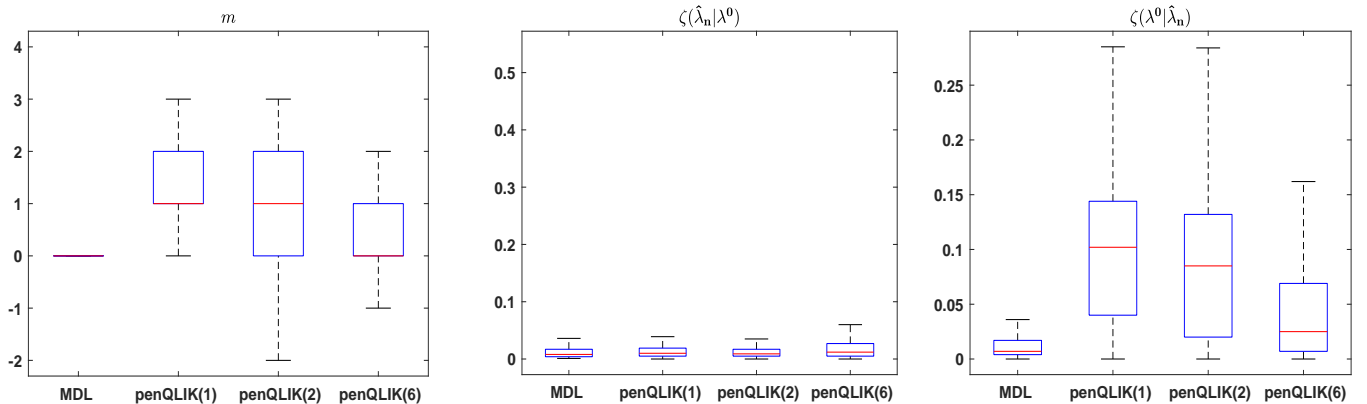


Figure 1: Boxplot of 1000 MDL, penQLIK(1), penQLIK(2) and penQLIK(6) simulations result for the Bias of the number of change-points estimator (left), the over-segmentation error(middle), the under-segmentation error (right) under the scenario MCP-NBINAR.

5.3 Consistency Analysis

In this section, we illustrate the “consistency”-like property of Auto-PGINARM-SA via studying the finite-sample performance on a range of simulated data. we choose BiINAR

and NBINAR process as GINAR processes within the MCP-GINAR models, and consider $m^0 = 1, 2, 3$ cases. The sample sizes considered are $n = 500, 1000$ and 1500 . For the generation of the j -th segment coefficient $\boldsymbol{\alpha}_j = (\alpha_{1,j}, \dots, \alpha_{p_j,j})$, we use the following steps. let $\tilde{\alpha}_j = \sum_{i=1}^{p_j} \alpha_{i,j}$, considering the condition $0 < \tilde{\alpha}_j < 1$, when we choose a specific $\tilde{\alpha}_j$, we use the "drchrnd" function in MATLAB to generate a list of random numbers $(\tilde{\alpha}_{1,j}, \dots, \tilde{\alpha}_{p_j,j})$, then use $\alpha_{i,j}^0 = \tilde{\alpha}_j * \tilde{\alpha}_{i,j}, i = 1, \dots, p_j$ as the j -th segment's true coefficient. All parameter settings and model definitions are summarized in Table 4.

Table 4: Parameters setting of different scenarios.

Scenarios	Parameter Setting												
	the j -th segment: $X_{t,j} = \alpha_{1,j} \circ X_{t-1,j} + \dots + \alpha_{p_j,j} \circ X_{t-p_j,j} + Z_{t,j}$, where $Z_{t,j}$ is Poisson random variables with parameter γ_j .												
MCP-BiINAR ₁	$m^0 = 1, \boldsymbol{\lambda}^0 = 0.4n, \boldsymbol{p}^0 = (1, 3), \boldsymbol{\theta}^0 = (\boldsymbol{\theta}_1^0, \boldsymbol{\theta}_2^0)$												
Segment	I: BiINAR(1)			II: BiINAR(3)									
	$\alpha_{1,1}^0$	γ_1^0	$\alpha_{1,2}^0$	$\alpha_{2,2}^0$	$\alpha_{3,2}^0$	γ_2^0							
	0.5	0.5	0.4877	0.0200	0.2923	1							
MCP-BiINAR ₂	$m^0 = 2, \boldsymbol{\lambda}^0 = (0.4n, 0.8n), \boldsymbol{p}^0 = (1, 3, 1), \boldsymbol{\theta}^0 = (\boldsymbol{\theta}_1^0, \boldsymbol{\theta}_2^0, \boldsymbol{\theta}_3^0)$												
Segment	I: BiINAR(1)			II: BiINAR(3)			III: BiINAR(1)						
	$\alpha_{1,1}^0$	γ_1^0	$\alpha_{1,2}^0$	$\alpha_{2,2}^0$	$\alpha_{3,2}^0$	γ_2^0	$\alpha_{1,3}^0$	γ_3^0					
	0.5	0.5	0.1264	0.1052	0.5684	1	0.4	2					
MCP-BiINAR ₃	$m^0 = 3, \boldsymbol{\lambda}^0 = (0.3n, 0.5n, 0.8n), \boldsymbol{p}^0 = (1, 3, 1, 4), \boldsymbol{\theta}^0 = (\boldsymbol{\theta}_1^0, \boldsymbol{\theta}_2^0, \boldsymbol{\theta}_3^0, \boldsymbol{\theta}_4^0)$												
Segment	I: BiINAR(1)			II: BiINAR(3)			III: BiINAR(1)			IV: BiINAR(4)			
	$\alpha_{1,1}^0$	γ_1^0	$\alpha_{1,2}^0$	$\alpha_{2,2}^0$	$\alpha_{3,2}^0$	γ_2^0	$\alpha_{1,3}^0$	γ_3^0	$\alpha_{1,4}^0$	$\alpha_{2,4}^0$	$\alpha_{3,4}^0$	$\alpha_{4,4}^0$	γ_4^0
	0.5	0.05	0.1524	0.2818	0.3658	1	0.2	2	0.0252	0.0502	0.5692	0.2054	3
Scenarios	Parameter Setting												
	the j -th segment: $X_{t,j} = \alpha_{1,j} * X_{t-1,j} + \dots + \alpha_{p_j,j} * X_{t-p_j,j} + Z_{t,j}$, where $Z_{t,j}$ is Geometric random variables with parameter $\gamma_j/(1 + \gamma_j)$.												
MCP-NBINAR ₁	$m^0 = 1, \boldsymbol{\lambda}^0 = 0.4n, \boldsymbol{p}^0 = (1, 3), \boldsymbol{\theta}^0 = (\boldsymbol{\theta}_1^0, \boldsymbol{\theta}_2^0)$												
Segment	I: NBINAR(1)			II: NBINAR(3)									
	$\alpha_{1,1}^0$	γ_1^0	$\alpha_{1,2}^0$	$\alpha_{2,2}^0$	$\alpha_{3,2}^0$	γ_2^0							
	0.5	0.5	0.4877	0.0200	0.2923	1							
MCP-NBINAR ₂	$m^0 = 2, \boldsymbol{\lambda}^0 = (0.4n, 0.8n), \boldsymbol{p}^0 = (1, 3, 1), \boldsymbol{\theta}^0 = (\boldsymbol{\theta}_1^0, \boldsymbol{\theta}_2^0, \boldsymbol{\theta}_3^0)$												
Segment	I: NBINAR(1)			II: NBINAR(3)			III: NBINAR(1)						
	$\alpha_{1,1}^0$	γ_1^0	$\alpha_{1,2}^0$	$\alpha_{2,2}^0$	$\alpha_{3,2}^0$	γ_2^0	$\alpha_{1,3}^0$	γ_3^0					
	0.5	0.5	0.1264	0.1052	0.5684	1	0.4	2					
MCP-NBINAR ₃	$m^0 = 3, \boldsymbol{\lambda}^0 = (0.3n, 0.5n, 0.8n), \boldsymbol{p}^0 = (1, 3, 1, 4), \boldsymbol{\theta}^0 = (\boldsymbol{\theta}_1^0, \boldsymbol{\theta}_2^0, \boldsymbol{\theta}_3^0, \boldsymbol{\theta}_4^0)$												
Segment	I: NBINAR(1)			II: NBINAR(3)			III: NBINAR(1)			IV: NBINAR(4)			
	$\alpha_{1,1}^0$	γ_1^0	$\alpha_{1,2}^0$	$\alpha_{2,2}^0$	$\alpha_{3,2}^0$	γ_2^0	$\alpha_{1,3}^0$	γ_3^0	$\alpha_{1,4}^0$	$\alpha_{2,4}^0$	$\alpha_{3,4}^0$	$\alpha_{4,4}^0$	γ_4^0
	0.5	0.5	0.4524	0.1818	0.1658	1	0.4	0.5	0.0252	0.1502	0.4692	0.1554	2

We implement sample path of six processes with $n = 500$ in Figure 2, where all change-points are represented by dotted lines in the figure. We find that under the same parameter values, it is easier to distinguish the change-points regions in MCP-BiINAR processes.

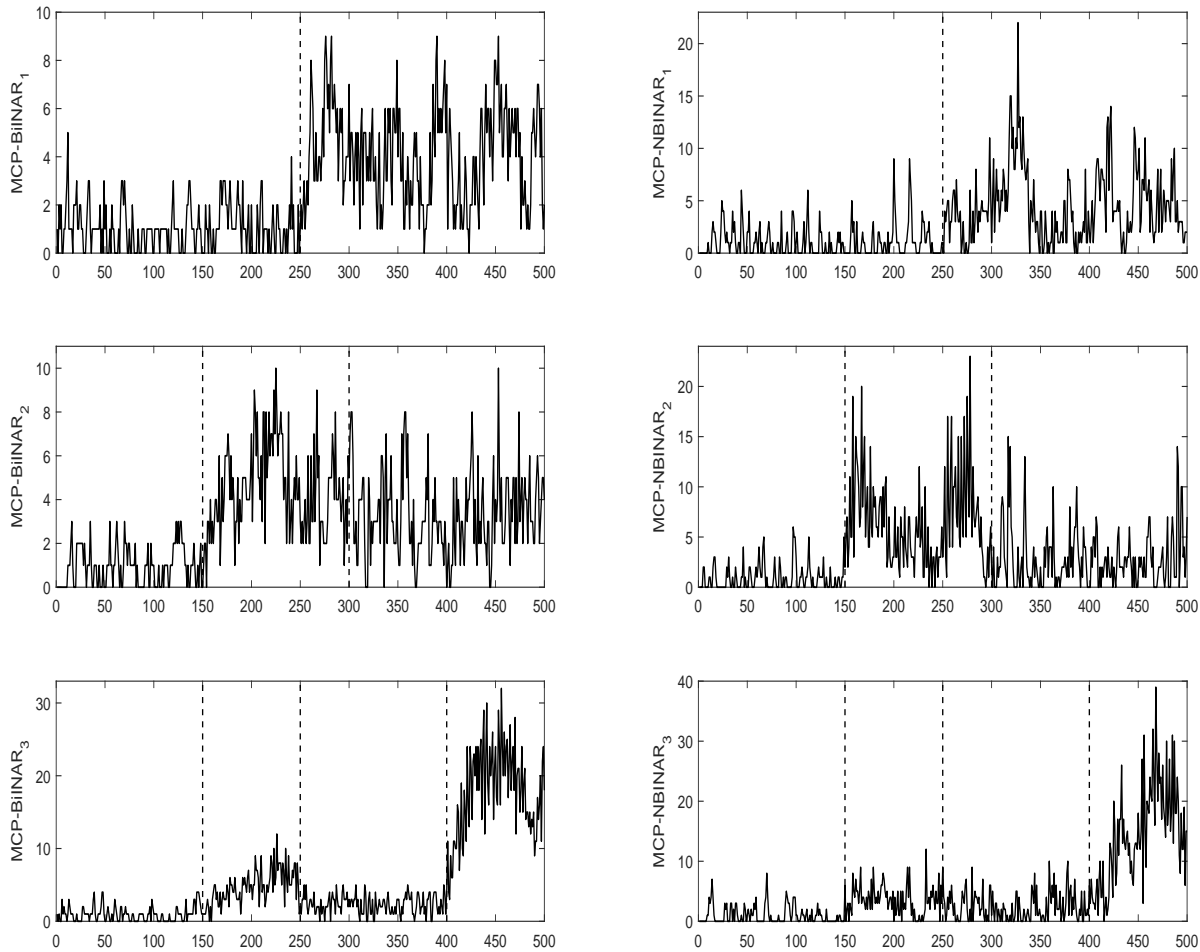


Figure 2: Sample paths plots of the scenarios MCP-BiINAR₁ to MCP-BiINAR₃. The dotted lines represent the location of the change-points.

To show a “consistency”-like property of Auto-PGINARM-SA, we split the simulation results into the following three parts:

(i) Table 5 and Table 6 indicates the frequencies of the true number of change-points and the MCP-GINAR order \mathbf{p} . As expected, the simulation results are quite satisfactory. Although some under-segmentation errors occur when $m^0 = 3$ and $n = 500$, with increasing sample size, the fraction of such “error” decreases. In general, for m and \mathbf{p} it is consistent with our conclusion in Section 3.

(ii) Table 7 indicates the Bias and MSE of the location of change-points when the number of change-points m is known. In addition, to evaluate the location accuracy of estimated change-points, we also report the distance from the estimated set $\hat{\lambda}_n$ and the true change-

point set $\boldsymbol{\lambda}^0$ under m is unknown,

$$d(\hat{\boldsymbol{\lambda}}_n, \boldsymbol{\lambda}^0) = \frac{1}{|\boldsymbol{\lambda}^0|} \sum_{\lambda_k^0 \in \boldsymbol{\lambda}^0} \min_{\hat{\lambda}_j \in \hat{\boldsymbol{\lambda}}_n} |\hat{\lambda}_j - \lambda_k^0| \quad (\text{Chen et al. (2021)}).$$

Table 7 shows that when m is known, the Bias and MSE of $\hat{\boldsymbol{\lambda}}_n$ are both quite minimal, which is a fantastic and satisfying effect and also supports the conclusion of our Theorem 1. On the other hand, it can be shown from $d(\hat{\boldsymbol{\lambda}}_n, \boldsymbol{\lambda}^0)$ that the distance considerably reduces with an increase in sample size, which is entirely compatible with the conclusion of consistency in Theorems 2 and 3.

(iii) Table 8 indicates the Bias and MSE of the estimator $\hat{\boldsymbol{\theta}}$. Considering that the distance between $\hat{\boldsymbol{\theta}}$ and $\boldsymbol{\theta}^0$ cannot be effectively defined when m is incorrectly estimated, we only look at the Bias and MSE of $\hat{\boldsymbol{\theta}}$ when m is correctly estimated. Tables 8 shows that the Bias and MSE of $\hat{\boldsymbol{\theta}}$ decrease as the sample size n increases. To gain more insight, we also present the QQ plots of the estimator $\hat{\boldsymbol{\theta}}$ for MCP-NBINAR₂ with sample size $n = 1500$ in Figure 3. The QQ plots show that the estimator $\hat{\boldsymbol{\theta}}$ is asymptotically normal, as predicted. Similar results are obtained for the remaining models, the figures are omitted to save space.

In conclusion, under all the scenarios, it is evident that the Auto-PGINARM-SA can solve the model selection problem of MCP-GINAR process effectively and perform more stable compared to other model selection method. This is consistent with our theoretical analysis in Section 3. Furthermore, it is worth noting that Auto-PGINARM-SA has superior efficiency for the case with MCP-BiINAR, since the PQML function is very close to its true likelihood function.

Table 5: Frequencies of the number of change-points estimated by the Auto-PGINARM-SA procedure for the scenarios MCP-BiINAR₁ to MCP-BiINAR₃.

Scenarios	n	Frequencies			Scenarios	n	Frequencies		
		$\hat{m} < m^0$	$\hat{m} = m^0$	$\hat{m} > m^0$			$\hat{m} < m^0$	$\hat{m} = m^0$	$\hat{m} > m^0$
MCP-BiINAR ₁	500	0	1	0	MCP-NBINAR ₁	500	0	0.954	0.046
$(m^0 = 1)$	1000	0	1	0	$(m^0 = 1)$	1000	0	0.982	0.018
	1500	0	1	0		1500	0	0.989	0.011
MCP-BiINAR ₂	500	0.099	0.901	0	MCP-NBINAR ₂	500	0.011	0.921	0.068
$(m^0 = 2)$	1000	0	1	0	$(m^0 = 2)$	1000	0	0.931	0.069
	1500	0	1	0		1500	0	0.933	0.067
MCP-BiINAR ₃	500	0.456	0.544	0	MCP-NBINAR ₃	500	0.44	0.542	0.018
$(m^0 = 3)$	1000	0.018	0.982	0	$(m^0 = 3)$	1000	0.032	0.949	0.019
	1500	0	1	0		1500	0.002	0.974	0.024

Table 6: Frequencies of the GINAR order estimated by the Auto-PGINARM-SA procedure for the scenarios MCP-BiINAR₁ to MCP-BiINAR₃.

Scenarios	n	Frequencies											
		$p_1^0 = 1$			$p_2^0 = 3$			$p_3^0 = 1$			$p_4^0 = 4$		
		$\hat{p}_1 < p_1^0$	$\hat{p}_1 = p_1^0$	$\hat{p}_1 > p_1^0$	$\hat{p}_2 < p_2^0$	$\hat{p}_2 = p_2^0$	$\hat{p}_2 > p_2^0$	$\hat{p}_3 < p_3^0$	$\hat{p}_3 = p_3^0$	$\hat{p}_3 > p_3^0$	$\hat{p}_4 < p_4^0$	$\hat{p}_4 = p_4^0$	$\hat{p}_4 > p_4^0$
MCP-BiINAR ₁ ($m^0 = 1$)	500	0	1	0	0.232	0.766	0.002						
	1000	0	0.998	0.002	0.013	0.987	0						
	1500	0	1	0	0.001	0.994	0.005						
MCP-BiINAR ₂ ($m^0 = 2$)	500	0	0.99	0.01	0.03	0.969	0.001	0.099	0.898	0.003			
	1000	0	0.999	0.001	0	0.999	0.001	0	0.997	0.003			
	1500	0	0.999	0.001	0	1	0	0	0.995	0.005			
MCP-BiINAR ₃ ($m^0 = 3$)	500	0	0.944	0.056	0.321	0.654	0.025	0.1	0.534	0.366	0.958	0.042	0
	1000	0	1	0	0.019	0.978	0.003	0	0.963	0.037	0.707	0.293	0
	1500	0	0.999	0.001	0.001	0.998	0.001	0	0.978	0.022	0.464	0.536	0
MCP-NBINAR ₁ ($m^0 = 1$)	500	0	0.99	0.01	0.062	0.918	0.02						
	1000	0	0.99	0.01	0.011	0.975	0.014						
	1500	0	0.991	0.009	0.006	0.977	0.017						
MCP-NBINAR ₂ ($m^0 = 2$)	500	0	0.982	0.018	0.012	0.973	0.015	0.011	0.95	0.039			
	1000	0	0.99	0.01	0.002	0.983	0.015	0	0.953	0.047			
	1500	0	0.982	0.018	0.001	0.987	0.012	0	0.945	0.055			
MCP-NBINAR ₃ ($m^0 = 3$)	500	0	0.677	0.323	0.534	0.395	0.071	0.286	0.477	0.237	0.892	0.107	0.001
	1000	0	0.956	0.044	0.487	0.501	0.012	0.009	0.875	0.116	0.54	0.454	0.006
	1500	0	0.989	0.011	0.314	0.672	0.014	0.001	0.908	0.091	0.354	0.637	0.009

Table 7: Summary of the change-points location estimated by the Auto-PGINARM-SA procedure for the scenarios MCP-BiINAR₁ to MCP-BiINAR₃.

Scenarios	n	$\hat{\lambda}_1$	$\hat{\lambda}_2$	$\hat{\lambda}_3$	$d(\hat{\lambda}_n, \lambda^0)$	Scenarios	n	$\hat{\lambda}_1$	$\hat{\lambda}_2$	$\hat{\lambda}_3$	$d(\hat{\lambda}_n, \lambda^0)$		
MCP-BiINAR ₁ ($m^0 = 1$)	500	Bias	0.0003		0.0377	MCP-NBINAR ₁ ($m^0 = 1$)	500	Bias	0.0018		0.0655		
		MSE	0.0002					MSE	0.0009				
	1000	Bias	-0.0006		0.0094	1000	Bias	0.0007		0.0140			
		MSE	0.0000				MSE	0.0001					
	1500	Bias	-0.0004		0.0043	1500	Bias	0.0008		0.0065			
		MSE	0.0000				MSE	0.0001					
MCP-BiINAR ₂ ($m^0 = 2$)	500	Bias	-0.0001	-0.0030	0.2974	MCP-NBINAR ₂ ($m^0 = 2$)	500	Bias	0.0028	0.0007	0.2900		
		MSE	0.0002	0.0006				MSE	0.0003	0.0016			
	1000	Bias	-0.0005	-0.0013	0.1500	1000	Bias	0.0013	-0.0007	0.1474			
		MSE	0.0000	0.0002			MSE	0.0001	0.0003				
	1500	Bias	-0.0004	-0.0005	0.0997	1500	Bias	0.0007	-0.0002	0.0983			
		MSE	0.0000	0.0001			MSE	0.0000	0.0001				
MCP-BiINAR ₃ ($m^0 = 3$)	500	Bias	0.0013	-0.0057	-0.0017	0.6056	MCP-NBINAR ₃ ($m^0 = 3$)	500	Bias	0.0068	-0.0042	0.0013	0.5851
		MSE	0.0002	0.0006	0.0001				MSE	0.0009	0.0008	0.0001	
	1000	Bias	0.0000	-0.0021	-0.0007	0.3037	1000	Bias	0.0020	-0.0020	0.0004	0.3005	
		MSE	0.0000	0.0002	0.0000			MSE	0.0002	0.0001	0.0000		
	1500	Bias	0.0000	-0.0015	-0.0004	0.2023	1500	Bias	0.0007	-0.0023	-0.0012	0.2008	
		MSE	0.0000	0.0001	0.0000			MSE	0.0001	0.0002	0.0004		

Table 8: Summary of parameter estimates obtained by Auto-PGINARM-SA procedure for the scenarios MCP-BiINAR₁ to MCP-BiINAR₃.

Segment		I		II				III		IV					
Scenarios	n		$\hat{\alpha}_{1,1}$	$\hat{\gamma}_1$	$\hat{\alpha}_{1,2}$	$\hat{\alpha}_{2,2}$	$\hat{\alpha}_{3,2}$	$\hat{\gamma}_2$	$\hat{\alpha}_{1,3}$	$\hat{\gamma}_3$	$\hat{\alpha}_{1,4}$	$\hat{\alpha}_{2,4}$	$\hat{\alpha}_{3,4}$	$\hat{\alpha}_{4,4}$	$\hat{\gamma}_4$
MCP-BiINAR ₁ ($m^0 = 1$)	500	Bias	-0.0132	0.0067	0.0083	0.0143	-0.0718	0.2704							
		MSE	0.0045	0.0051	0.0064	0.0031	0.0220	0.2946							
	1000	Bias	-0.0070	0.0043	-0.0042	0.0108	-0.0149	0.0743							
		MSE	0.0022	0.0027	0.0024	0.0013	0.0031	0.0529							
	1500	Bias	-0.0059	0.0034	-0.0007	0.0071	-0.0100	0.0471							
		MSE	0.0014	0.0017	0.0015	0.0009	0.0015	0.0300							
MCP-BiINAR ₂ ($m^0 = 2$)	500	Bias	-0.0214	0.0146	-0.0053	-0.0130	-0.0412	0.2698	-0.0135	0.0374					
		MSE	0.0073	0.0090	0.0050	0.0047	0.0074	0.3772	0.0049	0.0621					
	1000	Bias	-0.0140	0.0099	-0.0010	-0.0082	-0.0224	0.1297	-0.0065	0.0213					
		MSE	0.0038	0.0045	0.0026	0.0025	0.0033	0.1240	0.0023	0.0293					
	1500	Bias	-0.0072	0.0031	-0.0005	-0.0031	-0.0149	0.0659	-0.0035	0.0100					
		MSE	0.0022	0.0029	0.0016	0.0017	0.0020	0.0630	0.0015	0.0201					
MCP-BiINAR ₃ ($m^0 = 3$)	500	Bias	-0.0217	0.0173	0.0004	-0.0467	-0.0941	0.7004	-0.0201	0.0280	0.1997	0.0368	-0.0589	-0.1911	-0.1108
		MSE	0.0079	0.0094	0.0118	0.0164	0.0364	1.4724	0.0072	0.0568	0.0473	0.0070	0.0099	0.0392	1.1892
	1000	Bias	-0.0097	0.0039	0.0021	-0.0238	-0.0302	0.2197	-0.0091	0.0200	0.1447	0.0231	-0.0265	-0.1522	0.0171
		MSE	0.0032	0.0039	0.0053	0.0051	0.0071	0.2079	0.0032	0.0282	0.0262	0.0038	0.0041	0.0302	0.9130
	1500	Bias	-0.0066	0.0013	-0.0009	-0.0147	-0.0209	0.1628	-0.0071	0.0142	0.1110	0.0180	-0.0192	-0.1138	-0.0500
		MSE	0.0022	0.0028	0.0033	0.0033	0.0037	0.1206	0.0024	0.0199	0.0169	0.0027	0.0029	0.0209	0.7092
MCP-NBINAR ₁ ($m^0 = 1$)	500	Bias	-0.0280	0.0125	-0.0158	0.0165	-0.0271	0.1795							
		MSE	0.0075	0.0079	0.0057	0.0026	0.0074	0.1591							
	1000	Bias	-0.0136	0.0070	-0.0089	0.0126	-0.0118	0.0817							
		MSE	0.0039	0.0036	0.0026	0.0016	0.0026	0.0551							
	1500	Bias	-0.0082	0.0035	-0.0040	0.0076	-0.0091	0.0667							
		MSE	0.0025	0.0025	0.0018	0.0011	0.0017	0.0344							
MCP-NBINAR ₂ ($m^0 = 2$)	500	Bias	-0.0427	0.0165	-0.0148	-0.0207	-0.0534	0.3983	-0.0135	0.0298					
		MSE	0.0127	0.0126	0.0058	0.0048	0.0104	0.4833	0.0056	0.0894					
	1000	Bias	-0.0207	0.0110	-0.0113	-0.0100	-0.0235	0.1837	-0.0060	0.0087					
		MSE	0.0058	0.0063	0.0033	0.0026	0.0042	0.1440	0.0029	0.0420					
	1500	Bias	-0.0156	0.0041	-0.0033	-0.0069	-0.0204	0.1161	-0.0033	0.0021					
		MSE	0.0042	0.0041	0.0018	0.0017	0.0030	0.0866	0.0019	0.0296					
MCP-NBINAR ₃ ($m^0 = 3$)	500	Bias	-0.0550	0.0320	-0.0367	-0.0395	-0.0986	0.9187	-0.0467	0.0400	0.0623	-0.0143	-0.0594	-0.1151	1.0320
		MSE	0.0137	0.0138	0.0203	0.0173	0.0226	1.6163	0.0157	0.0711	0.0106	0.0090	0.0148	0.0204	3.0663
	1000	Bias	-0.0191	0.0069	-0.0020	-0.0031	-0.0635	0.3124	-0.0180	0.0104	0.0432	-0.0078	-0.0267	-0.0737	0.5681
		MSE	0.0062	0.0059	0.0083	0.0093	0.0159	0.3099	0.0060	0.0053	0.0057	0.0047	0.0052	0.0135	1.1605
	1500	Bias	-0.0179	0.0071	-0.0035	-0.0008	-0.0407	0.1833	-0.0148	0.0073	0.0325	-0.0034	-0.0212	-0.0507	0.3659
		MSE	0.0043	0.0039	0.0051	0.0055	0.0104	0.1270	0.0043	0.0033	0.0040	0.0032	0.0033	0.0094	0.6941

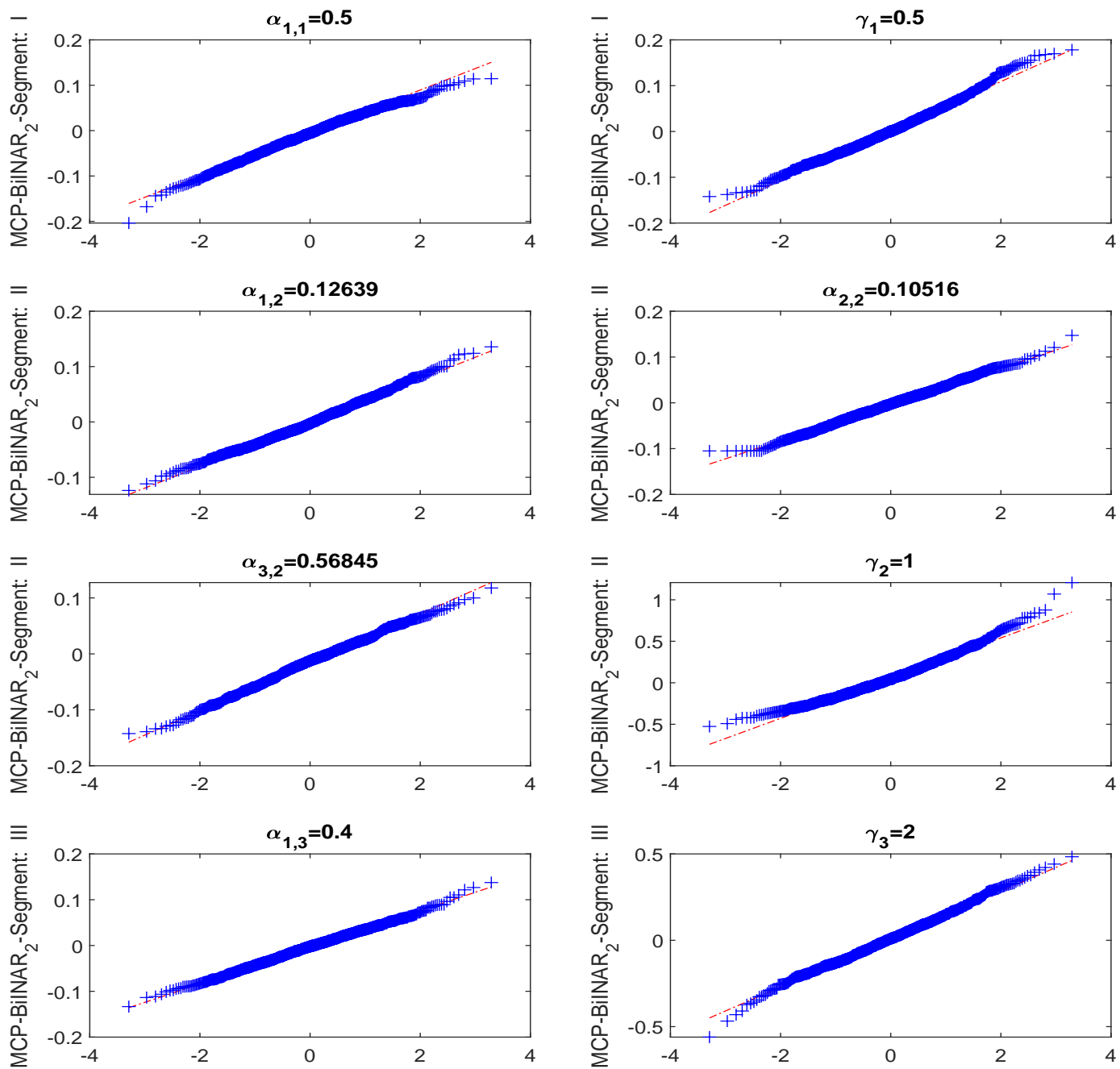


Figure 3: QQ plots of the parameter θ estimator for the scenario MCP-NBINAR₂ with sample size $n = 1500$.

6 Real data

In this section, we apply the proposed Auto-PGINARM-SA procedure to identify changes in three examples of real data series.

6.1 Poilo data

Firstly, we consider the monthly cases of poliomyelitis data in the US for a period of 14 years from 1970 to 1983 (see Figure 4). There are 168 observations reported by the Centers for Disease Control and Prevention and have already been analyzed by several authors. By investigating the autocorrelation function (ACF) and partial ACF plots from the data and by observing the spikes, Zheng et al. (2006) proposed that RCINAR(1) model could be used to fit this set of data. Furthermore, Kang and Lee (2009) demonstrated by cumulative sum (CUSUM) that there exist change-point in these data, and obtained that the change-point location was the 35th observation point through the position where the statistics reached the maximum value.

In this subsection, we apply the Auto-PGINARM-SA procedure to determine the location of the change-point and the corresponding parameters, and finally get the following MCP-GINAR estimated model,

$$E(X_t|\mathcal{F}_{t-1}) \begin{cases} 0.2332X_{t-1,1} + 1.8183, & 0 < t \leq 35, \\ (0.2279) \quad (0.4051) \\ 0.2855X_{t-1,2} + 0.7574, & 36 \leq t \leq 168. \\ (0.1313) \quad (0.1111) \end{cases}$$

where in parentheses are the standard errors (SE) of the estimators obtained from the square roots of the elements in the diagonal of the matrix $\hat{\Sigma}_j = \hat{\mathbf{J}}_j^{-1} \hat{\mathbf{I}}_j \hat{\mathbf{J}}_j^{-1}$ computed on each segment j , with $\hat{\mathbf{J}}_j$ and $\hat{\mathbf{I}}_j$ are given by (2.3) - (2.4). The results show that there is a change-point in this data set, and the change-point location is $\hat{\tau}_1 = 35$ (see Figure 4). This is consistent with the results of Kang and Lee (2009).

6.2 Technofirst stock trades data

Secondly, we consider the daily number of trades in the stock of Technofirst listed in the NYSE Euronext group. This data set consists of 1662 observations from August 13, 2003 to December 3, 2013, and is available on the website “<https://www.euronext.com/en/products/equities/FR0011651819-ALXP>”. Also, these data have been analyzed by many scholars. For example, Ahmad and Francq (2016) analyzed six stocks data listed in the NYSE Euronext group, including CR.FONC.MONACO, Siraga, Technofirst, Siparex Croissance, Proximedia and Achmea. From their times series and ACF figures, it is not difficult to see that the stock trading data of Siraga, Technofirst, Siparex Crolssance and Achmea are all poissble to have change-points. Furthermore, Diop and Kengne (2021b) analyzed part of the data in Technofirst (corresponding to 1020-1662 of the data analyzed by us) and confirmed

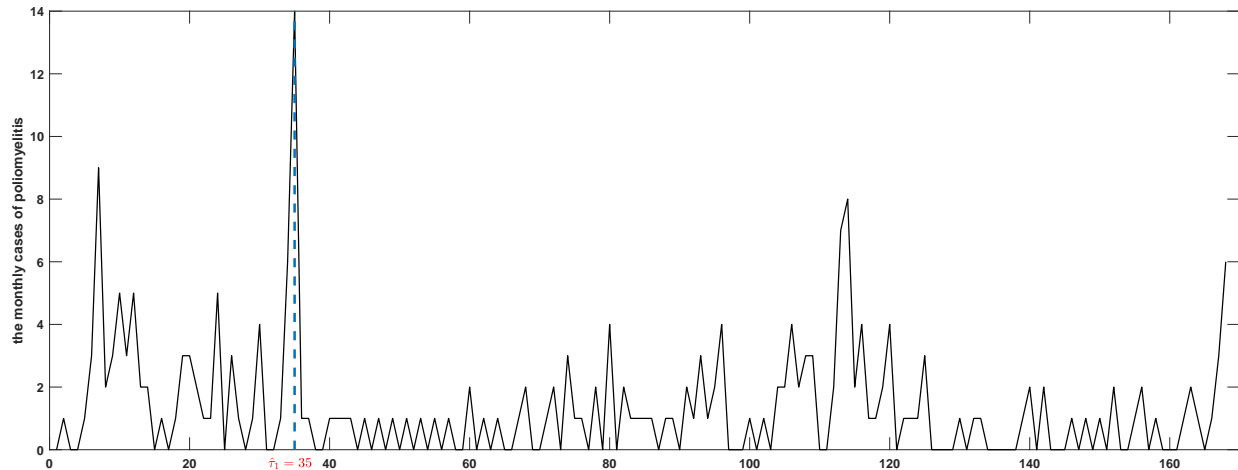


Figure 4: Sample path of the monthly cases of poliomyelitis data.
The dotted line represents the estimated location of the change-point $\hat{\tau}_1$.

the existence of change-points. They got the locations of change-points are 230 and 311 (corresponding to 1249 and 1330 in our data).

In this subsection, we also apply the proposed Auto-PGINARM-SA procedure to this financial time series data. Figure 5 shows the time series and the estimated locations of change-points. Through the Auto-PGINARM-SA procedure, the number of change-points $\hat{m} = 6$, the change-points locations $\hat{\tau} = \{110, 390, 491, 564, 1246, 1330\}$ are obtained, and the corresponding estimated model is as follows:

$$E(X_t | \mathcal{F}_{t-1}) = \begin{cases} 0.2922X_{t-1,1} + 1.0038, & 0 < t \leq 110, \\ (0.1096) & (0.1632) \\ 0.1572X_{t-1,2} + 2.1611, & 111 \leq t \leq 390, \\ (0.0746) & (0.1880) \\ 0.1523X_{t-1,3} + 3.7013, & 391 \leq t \leq 491, \\ (0.0874) & (0.4299) \\ 0.6099X_{t-1,4} + 3.2385, & 492 \leq t \leq 564, \\ (0.1902) & (1.7358) \\ 0.3161X_{t-1,5} + 2.5951, & 565 \leq t \leq 1246, \\ (0.0438) & (0.1687) \\ 0.6661X_{t-1,6} + 4.2140, & 1247 \leq t \leq 1330, \\ (0.1124) & (1.3606) \\ 0.2182X_{t-1,7} + 3.0588, & 1331 \leq t \leq 1662. \\ (0.0732) & (0.2917) \end{cases}$$

It can be seen that the change-points locations 1246 and 1330 obtained by using the Auto-PGINARM-SA procedure are consistent with 1249 and 1330 obtained by [Diop and Kengne \(2021b\)](#). This shows that our proposed model and method can also effectively analyze the locations of change-points. However, the SE of the estimators in segments 4 and 6 were observed to be insignificant, some other models, such as INGARCH models, should be considered to fit the data in these two segments in future studies.

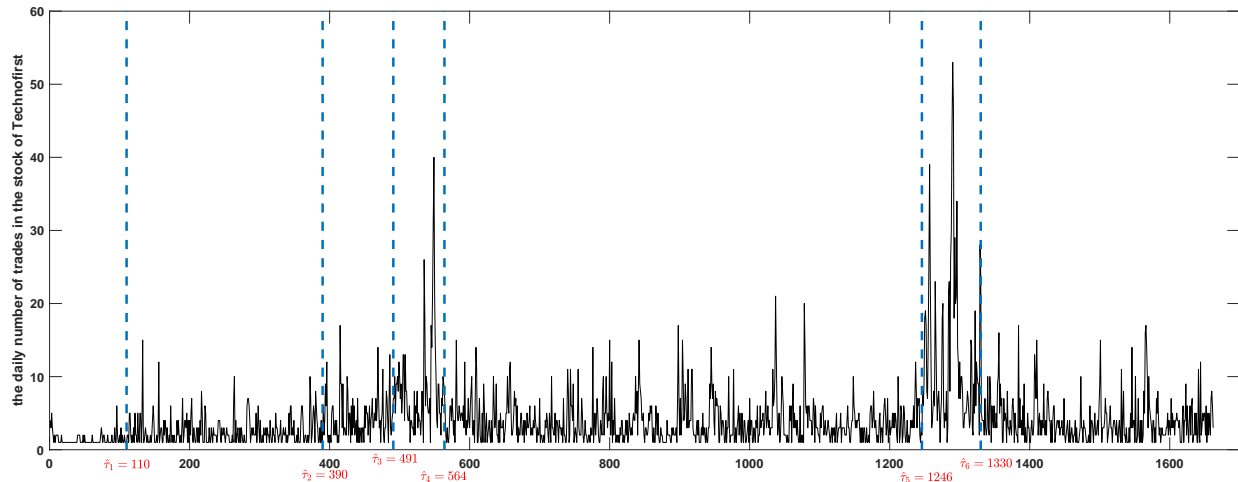


Figure 5: Sample path of the daily number of trades in the stock of Technofirst data. The dotted lines represent the estimated locations of the change-points $\hat{\tau}_1 - \hat{\tau}_6$.

6.3 Siraga stock trades data

In this subsection, we consider another financial time series data, that is, the daily number of trades in the stock of Siraga listed in the NYSE Euronext group. This data set consists of 2362 observations and is available on the website “<https://live.euronext.com/en/product/equities/FR0000060170-XPAR>”. Similar to the previous two applications, Figure 6 shows the time series and the estimated locations of change-points. Through the Auto-PGINARM-SA procedure, we obtained the number of change-points $\hat{m} = 6$, the change-points locations $\hat{\tau} = \{266, 894, 1305, 1992, 2278, 2362\}$, and the corresponding estimated model is as follows:

$$E(X_t | \mathcal{F}_{t-1}) = \begin{cases} 0.0610X_{t-1,1} + 0.1144X_{t-2,1} + 0.0001X_{t-3,1} + 0.1273X_{t-4,1} + 0.2038X_{t-5,1} + 1.7422, & 0 < t \leq 266, \\ (0.0538) & (0.0611) & (0.0637) & (0.0635) & (0.0658) & (0.3327) \\ 0.2061X_{t-1,2} + 1.3324, & & & & & & 267 \leq t \leq 894, \\ (0.0438) & (0.0792) & & & & & \\ 0.0998X_{t-1,3} + 2.5934, & & & & & & 895 \leq t \leq 1305, \\ (0.0495) & (0.1573) & & & & & \\ 0.1234X_{t-1,4} + 0.2269X_{t-2,4} + 3.0545, & & & & & & 1306 < t \leq 1666, \\ (0.0540) & (0.0617) & (0.4524) & & & & \\ 0.3352X_{t-1,5} + 1.7640, & & & & & & 1667 \leq t \leq 1992, \\ (0.0609) & (0.1554) & & & & & \\ 0.2007X_{t-1,6} + 4.0554, & & & & & & 1993 \leq t \leq 2278, \\ (0.0537) & (0.3484) & & & & & \\ 0.0001X_{t-1,7} + 2.2458, & & & & & & 2279 \leq t \leq 2362. \\ (0.1041) & (0.2359) & & & & & \end{cases}$$

Clearly, all estimators of the estimated MCP-GINAR model except the last segment are significant regarding the standard errors. For the last segment, judging from the results, it seems more appropriate to fit it with the integer-valued moving average (INMA) model.

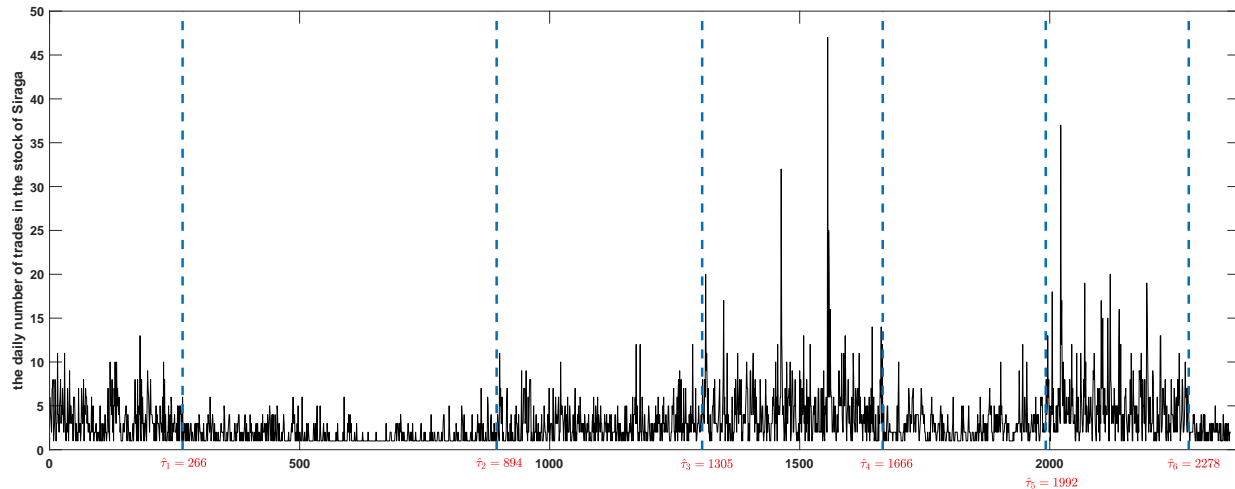


Figure 6: Sample path of the daily number of trades in the stock of Siraga data. The dotted lines represent the estimated locations of the change-points $\hat{\tau}_1 - \hat{\tau}_6$.

7 Conclusion and discussion

This paper introduces a piecewise stationary model, MCP-GINAR, to describe the common non-stationary processes in statistics. The MDL criterion based on the PQML for the MCP-GINAR model has been proposed to estimate the number of change-points, the location of the change-points, the order of each segment and its parameters. Regarding the consistency of the MDL model selection procedure, we reach the following conclusions. When the number of change-points is known, if $E|X_{t,j}|^{2+\eta} < \infty$, estimators based on MDL procedure are strongly consistent. Under the condition of the number of change-points is unknown, if $E|X_{t,j}|^{4+\eta} < \infty$, estimators are weakly consistent, further, if $E|X_{t,j}|^{8+\eta} < \infty$, estimators are strongly consistent. Regarding optimizing MDL, an improved genetic algorithm with simulated annealing, Auto-PGINARM-SA, is proposed. The simulation results in Section 5 show that the Auto-PGINARM-SA program is very satisfactory. It can not only find solutions, but also effectively solve the precocious problem of the genetic algorithm. Finally, we use Auto-PGINARM-SA to complete the change-points estimation analysis for three applications, and the analysis results indicate that the proposed procedure is useful in practice.

However, we must point out that there are many topics that are worth further research. On the one hand, the extension of the MCP-GINAR model will be an important issue. As the results of the second and third applications in Section 6 show, although the Auto-PGINARM-SA procedure can effectively solve the change-points estimation problem, some other models, such as INGARCH models, INMA models, may be more suitable to fit the data. So extending the MCP-GINAR(\mathbf{p}) model to MCP-INGARCH(\mathbf{p}, \mathbf{q}) will be an interesting topic. On the other hand, the optimization of MDL will be a popular topic for MCP-GINAR, such as Dynamic Programming, Optimal Partitioning, Pruned Exact Linear Time algorithms are all

worth trying. We will leave the above issues as our future work.

Acknowledgements

This work is supported by National Natural Science Foundation of China (No.12271231, 12001229, 11901053).

Appendix

As stated in Section 3, in practice, the observed likelihood $\tilde{L}_{n_j}^{(j)}(\boldsymbol{\theta}_j; p_j, \mathbf{x}_j)$ is used to approximate the true likelihood $L_{n_j}^{(j)}(\boldsymbol{\theta}_j; p_j, \mathbf{x}_j)$, so let us first state the following Lemma to control this approximation. Also, this Lemma will be used to prove all theorems.

Lemma 1 *Let $\{X_t\}$ be a piecewise stationary process MCP-GINAR process defined in (1.2). If $E(X_{t,j})^{2k+\eta} < \infty$ for some $\eta > 0$, then the Assumption 1 (k) in Davis and Yau (2013) can be verified. That is, for any $j = 1, 2, \dots, m+1$ and fixed p_j , the function $\ell_t^{(j)}$ is two-time continuously differentiable with respect to $\boldsymbol{\theta}_j$ and the first and second derivatives $L_{n_j}^{(j)}$, $\tilde{L}_{n_j}^{(j)}$ and $L_{n_j}^{\prime(j)}$, $\tilde{L}_{n_j}^{\prime(j)}$, respectively, of the function defined in (2.2) and (3.1), satisfy*

$$\sup_{\boldsymbol{\theta}_j \in \Theta_j(p_j)} \left| \frac{1}{n} L_{n_j}^{(j)}(\boldsymbol{\theta}_j; p_j, \mathbf{x}_j) - \frac{1}{n} \tilde{L}_{n_j}^{(j)}(\boldsymbol{\theta}_j; p_j, \mathbf{x}_j) \right| = o(n^{\frac{1}{k}-1}), \quad (7.1)$$

$$\sup_{\boldsymbol{\theta}_j \in \Theta_j(p_j)} \left| \frac{1}{n} L_{n_j}^{\prime(j)}(\boldsymbol{\theta}_j; p_j, \mathbf{x}_j) - \frac{1}{n} \tilde{L}_{n_j}^{\prime(j)}(\boldsymbol{\theta}_j; p_j, \mathbf{x}_j) \right| = o(n^{\frac{1}{k}-1}), \quad (7.2)$$

$$\sup_{\boldsymbol{\theta}_j \in \Theta_j(p_j)} \left| \frac{1}{n} L_{n_j}^{\prime\prime(j)}(\boldsymbol{\theta}_j; p_j, \mathbf{x}_j) - \frac{1}{n} \tilde{L}_{n_j}^{\prime\prime(j)}(\boldsymbol{\theta}_j; p_j, \mathbf{x}_j) \right| = o(1), \quad (7.3)$$

almost surely.

Proof of Lemma 1. We first prove (7.1),

$$\begin{aligned} & |L_{n_j}^{(j)}(\boldsymbol{\theta}_j; p_j, \mathbf{x}_j) - \tilde{L}_{n_j}^{(j)}(\boldsymbol{\theta}_j; p_j, \mathbf{x}_j)| \\ &= \left| \sum_{t=1}^{n_j} X_{t,j} \log \left(\frac{\xi_{t,j}(\boldsymbol{\theta}_j; p_j | X_{s,j}, s < t)}{\xi_{t,j}(\boldsymbol{\theta}_j; p_j | \tilde{\mathbf{x}}_{i,j})} \right) - [\xi_{t,j}(\boldsymbol{\theta}_j; p_j | X_{s,j}, s < t) - \xi_{t,j}(\boldsymbol{\theta}_j; p_j | \tilde{\mathbf{x}}_{i,j})] \right| \\ &\leq \sum_{t=1}^{n_j} \left(\left| X_{t,j} \log(v_{t,j}^{(1)}) \right| + \left| v_{t,j}^{(2)} \right| \right), \end{aligned}$$

where

$$v_{t,j}^{(1)} = \frac{\sum_{k=1}^{p_j} \alpha_{k,j} X_{t-k,j} + \gamma_j}{\sum_{k=1}^{p_j} \alpha_{k,j} X_{\tau_{j-1}+t-k} + \gamma_j}, \quad v_{t,j}^{(2)} = \sum_{k=1}^{p_j} \alpha_{k,j} (X_{t-k,j} - X_{\tau_{j-1}+t-k}).$$

Since $\alpha_{k,j} \in (0, 1)$ and $\gamma_j > 0$, there exist a suitable constant $0 < C_1 < \infty$ satisfy $|\log(v_{t,j}^{(1)})| \leq C_1 X_{t,j}$, thus,

$$|L_{n_j}^{(j)}(\boldsymbol{\theta}_j; p_j, \mathbf{x}_j) - \tilde{L}_{n_j}^{(j)}(\boldsymbol{\theta}_j; p_j, \mathbf{x}_j)| \leq \sum_{t=1}^{n_j} \left(C_1 |X_{t,j}|^2 + |v_{t,j}^{(2)}| \right).$$

Note that when $E(X_{t,j})^{2k} < \infty$, from Borel-Cantelli lemma, for any $K > 0$,

$$\begin{aligned} \sum_{t=1}^{n_j} P(X_{t,j}^2 > Kn^{\frac{1}{k}}) &= \sum_{t=1}^{n_j} P(X_{t,j}^{2k} > K^k n) \leq \frac{1}{K^k} E(X_{t,j})^{2k} < \infty, \\ \sum_{t=1}^{n_j} P(|v_{t,j}^{(2)}| > Kn^{\frac{1}{k}}) &= \sum_{t=1}^{n_j} P(|v_{t,j}^{(2)}|^k > K^k n) \leq \frac{1}{K^k} E|v_{t,j}^{(2)}|^k < \infty, \end{aligned}$$

thus when $E(X_{t,j})^{2k+\eta} < \infty$, we have $\sum_{t=1}^{n_j} \left(C_1 |X_{t,j}|^2 + |v_{t,j}^{(2)}| \right) = o(n^{\frac{1}{k}})$ almost surely. In the similar way, (7.2) and (7.3) hold if $E(X_{t,j})^{2k+\eta} < \infty$. The proof of Lemma 1 is completed.

Next, we use the following Lemma to illustrate some conditions of PQML function, which are also conditions for the consistency and asymptotic normality of the PQML estimator in Ahmad and Francq (2016).

Lemma 2 *Let $\{X_t\}$ be a piecewise stationary MCP-GINAR process defined in (1.2). If $E(X_{t,j})^{2k+\eta} < \infty$ for some $\eta > 0$, then the Assumption 2 (k) in Davis and Yau (2013) can be verified. That is, for any $j = 1, 2, \dots, m+1$ and fixed p_j , there exists an $\epsilon > 0$ such that*

$$\sup_{\boldsymbol{\theta}_j \in \Theta_j(p_j)} E|\ell_t^{(j)}(\boldsymbol{\theta}_j; p_j, X_{t,j}|X_{s,j}, s < t)|^{k+\epsilon} < \infty, \quad (7.4)$$

$$\sup_{\boldsymbol{\theta}_j \in \Theta_j(p_j)} E|\ell_t^{\prime(j)}(\boldsymbol{\theta}_j; p_j, X_{t,j}|X_{s,j}, s < t)|^{k+\epsilon} < \infty, \quad (7.5)$$

$$\sup_{\boldsymbol{\theta}_j \in \Theta_j(p_j)} E|\ell_t^{\prime\prime(j)}(\boldsymbol{\theta}_j; p_j, X_{t,j}|X_{s,j}, s < t)| < \infty, \quad (7.6)$$

where $\ell_t^{\prime(j)}$ and $\ell_t^{\prime\prime(j)}$ are the first and second derivatives of $\ell_t^{(j)}$, $\ell_t^{(j)}(\boldsymbol{\theta}_j; p_j, X_{t,j}|X_{s,j}, s < t)$ is defined in (2.2).

Proof of Lemma 2. $\ell_t^{(j)}$ and its first and second derivatives are given by

$$\begin{aligned} \ell_t^{(j)}(\boldsymbol{\theta}_j; p_j, X_{t,j}|X_{s,j}, s < t) &= X_{t,j} \log \xi_{t,j}(\boldsymbol{\theta}_j; p_j|X_{s,j}, s < t) - \xi_{t,j}(\boldsymbol{\theta}_j; p_j, |X_{s,j}, s < t), \\ \ell_t^{\prime(j)}(\boldsymbol{\theta}_j; p_j|X_{s,j}, s < t) &= \frac{1}{\xi_{t,j}(\boldsymbol{\theta}_j)} \frac{\partial \xi_{t,j}(\boldsymbol{\theta}_j)}{\partial \boldsymbol{\theta}_j} \frac{\partial \xi_{t,j}(\boldsymbol{\theta}_j)}{\partial \boldsymbol{\theta}_j^T}, \\ \ell_t^{\prime\prime(j)}(\boldsymbol{\theta}_j; p_j|X_{s,j}, s < t) &= \left(\frac{X_{t,j}}{\xi_{t,j}(\boldsymbol{\theta}_j)} - 1 \right)^2 \frac{\partial \xi_{t,j}(\boldsymbol{\theta}_j)}{\partial \boldsymbol{\theta}_j} \frac{\partial \xi_{t,j}(\boldsymbol{\theta}_j)}{\partial \boldsymbol{\theta}_j^T}. \end{aligned}$$

By the same arguments as the Lemma 1, there exist a suitable constant $0 < C_2 < \infty$ satisfy $E|\ell_t^{(j)}(\boldsymbol{\theta}_j; p_j, X_{t,j}|X_{s,j}, s < t)| \leq C_2 E(X_{t,j})^2$, thus (7.4) holds if $E(X_{t,j})^{2k+\eta} < \infty$. On the

other hand, according to the arguments in Section 3.7. of [Ahmad and Francq \(2016\)](#), we have

$$\begin{aligned}\ell_t^{(j)'}(\boldsymbol{\theta}_j; p_j, X_{t,j}|X_{s,j}, s < t) &\leq C_3 + C_4 X_{t,j}, \\ \ell_t^{(j)''}(\boldsymbol{\theta}_j; p_j, X_{t,j}|X_{s,j}, s < t) &\leq C_5(C_3 + C_4 X_{t,j}),\end{aligned}$$

where C_3, C_4, C_5 are some suitable constants. Thus if $E(X_{t,j})^{2k+\eta} < \infty$, then (7.5) and (7.6) can be verified.

Proof of Theorem 1. In order to prove Theorem 1, it is sufficient to show that Assumptions 1 (1), 2 (1) and 3 of [Davis and Yau \(2013\)](#) holds. Note that if we take $k = 1$, that is $E(X_{t,j})^{2+\eta} < \infty$, Assumptions 1 (1), 2 (1) are satisfied according to Lemma 1 and 2. Assumption 3 can be verified by the ergodic theorem and the compactness of the parameter space. The proof of Theorem 1 is completed.

Proof of Theorem 2. For Theorem 2 to hold we verify Assumptions 1 (1), 1*, 2 (2), 3 and 5 in [Davis and Yau \(2013\)](#). Similar to the argument in the proof of Theorem 1, if the $(2 * 2 + \eta)$ -th moment of $X_{t,j}$ exists, then Assumptions 1 (1), 1*, 2 (2) and 3 hold. Next we verify that Assumption 5 holds. Considering that $\boldsymbol{\theta}_j$ belongs to the interior of $\Theta_j(p_j)$ Assumption 5A) is easily demonstrated for GINAR(p_j) process according to PQML in [Ahmad and Francq \(2016\)](#). On the other hand, GINAR(p_j) can be written as an AR(p_j) process according to Remark 2. Similar to the arguments of Example 2 in [Davis and Yau \(2013\)](#), we can verify that Assumption 5B) holds. Thus the proof of Theorem 2 is completed.

Proof of Theorem 3. For Theorem 3 to hold we verify Assumptions 1 (2), 2 (4), 3, 5, and either 4 (0.5) or 4* in [Davis and Yau \(2013\)](#). Similar to the argument in the proof of Theorem 2, if the $(2 * 4 + \eta)$ -th moment of $X_{t,j}$ exists, then Assumptions 1 (2), 2 (4), 3 and 5 hold. Therefore, it remains to verify Assumption 4 (0.5) or 4*. It is well known that GINAR(p_j) process is a stationary ergodic Markov chain according to Remark 1, that is, GINAR(p_j) process is strongly mixing with geometric rate. Also, GINAR(p_j) can be written as an AR(p_j) process according to Remark 2. Thus $\ell_t^{(j)'}(\boldsymbol{\theta}_j; p_j, X_{t,j}|X_{s,j}, s < t)$ is strongly mixing with the same geometric rate as it is a function of finite number of the strongly mixing $X_{t,j}$'s (Theorem 14.1 of [Davidson \(1994\)](#)). Thus Assumption 4* holds. In fact, Lemma 1 in [Davis and Yau \(2013\)](#) already states that Assumption 4(0.5) holds under Assumption 2(2) and 4*. Note that Assumption 2(2) is obviously satisfied under $E(X_{t,j})^{8+\eta} < \infty$. Therefore, Assumption 4(0.5) is also satisfied under our assumptions. The proof of Theorem 3 is completed.

References

- Ahmad, A., Francq, C. (2016). Poisson QMLE of count time series models. *Journal of Time Series Analysis*, 37(3), 291-314.
- Al-Osh, M.A., Alzaid, A.A. (1987). First-order integer-valued autoregressive (INAR(1)) process. *Journal of Time Series Analysis*, 8, 261-275.

- Aue, A., Horváth, L. (2013). Structural breaks in time series. *Journal of Time Series Analysis*, 34, 1-16.
- Aue, A., Cheung, R. C., Lee, T. C., and Zhong, M. (2014). Segmented model selection in quantile regression using the minimum description length principle. *Journal of the American Statistical Association*, 109(507), 1241-1256.
- Barreto-Souza, W. (2019). Mixed Poisson INAR(1) processes. *Statistical Papers*, 60, 2119-2139.
- Baudry, J. P., Maugis, C., Michel, B. (2012). Slope heuristics: overview and implementation. *Statistics and Computing*, 22, 455-470.
- Boysen, L., Kempe, A., Liebscher, V., Munk, A., and Wittich, O. (2009). Consistencies and rates of convergence of jump-penalized least squares estimators. *The Annals of Statistics*, 37(1), 157-183.
- Bu, R., McCabe, B., Hadri, K. (2008). Maximum likelihood estimation of higher-order integer-valued autoregressive processes. *Journal of time series analysis*, 29(6), 973-994.
- Casini, A., Perron, P. (2018). Structural breaks in time series. *arXiv preprint arXiv:1805.03807*.
- Chan, N. H., Yau, C. Y., Zhang, R. M. (2014). Group LASSO for structural break time series. *Journal of the American Statistical Association*, 109(506), 590-599.
- Chattopadhyay, S., Maiti, R., Das, S., and Biswas, A. (2021). Change-point analysis through integer-valued autoregressive process with application to some COVID-19 data. *Statistica Neerlandica*, 76, 4-34.
- Chen, H., Ren, H., Yao, F., and Zou, C. (2021). Data-driven selection of the number of change-points via error rate control. *Journal of the American Statistical Association*, 1-14.
- Darolles, S., Le Fol, G., Lu, Y., and Sun, R. (2019). Bivariate integer-autoregressive process with an application to mutual fund flows. *Journal of Multivariate Analysis*, 173, 181-203.
- Davis, R. A., Hancock, S. A., Yao, Y. C. (2016). On consistency of minimum description length model selection for piecewise autoregressions. *Journal of Econometrics*, 194(2), 360-368.
- Davis, R. A., Lee, T. C. M., Rodriguez-Yam, G. A. (2006). Structural break estimation for nonstationary time series models. *Journal of the American Statistical Association*, 101(473), 223-239.
- Davis, R. A., Yau, C. Y. (2013). Consistency of minimum description length model selection for piecewise stationary time series models. *Electronic Journal of Statistics*, 7, 381-411.
- Davidson, J. (1994). *Stochastic Limit Theory*. Oxford: Oxford University Press.
- Diop, M. L., Kengne, W. (2021a). Epidemic change-point detection in general integer-valued time series. *arXiv preprint arXiv:2103.13336*.
- Diop, M. L., Kengne, W. (2021b). Piecewise autoregression for general integer-valued time series. *Journal of Statistical Planning and Inference*, 211, 271-286.

- Diop, M. L., Kengne, W. (2022). Poisson QMLE for change-point detection in general integer-valued time series models. *Metrika*, 85(3), 373-403.
- Doerr, B., Fischer, P., Hilbert, A., and Witt, C. (2017). Detecting structural breaks in time series via genetic algorithms. *Soft Computing*, 21, 4707-4720.
- Fernández-Fontelo, A., Cabaña, A., Puig, P., and Moriña, D. (2016). Under-reported data analysis with INAR-hidden Markov chains. *Statistics in Medicine*, 35, 4875-4890.
- Fernández-Fontelo, A., Cabaña, A., Joe, H., Puig, P., and Moriña, D. (2021). Untangling serially dependent underreported count data for gender-based violence. *Statistics in Medicine*, 38, 4404-4422.
- Gourieroux, C., Jasiak, J. (2004). Heterogeneous INAR (1) model with application to car insurance. *Insurance: Mathematics and Economics*, 34, 177-192.
- Guan, G., Hu, X. (2022). On the analysis of a discrete-time risk model with INAR (1) processes. *Scandinavian Actuarial Journal*, 2022, 115-138.
- Henderson, N.C., Rathouz, P.J. (2018). AR(1) latent class models for longitudinal count data. *Statistics in Medicine*, 37, 4441-4456.
- Jong, K., Marchiori, E., Van Der Vaart, A., Ylstra, B., Weiss, M., and Meijer, G. (2003). Chromosomal breakpoint detection in human cancer. 2003 *Applications of Evolutionary Computing: EvoWorkshops 2003: EvoBIO, EvoCOP, EvoIASP, EvoMUSART, EvoROB, and EvoSTIM*, Volume 2611 of LNCS, University of Essex, England, UK. Springer-Verlag, Berlin, pp. 54-65.
- Kang, J., Lee, S. (2009). Parameter change test for random coefficient integer-valued autoregressive processes with application to polio data analysis. *Journal of Time Series Analysis*, 30, 239-258.
- Kirkpatrick, S., Gelatt Jr, C. D., Vecchi, M. P. (1983). Optimization by simulated annealing. *science*, 220(4598), 671-680.
- Latour, A. (1998). Existence and stochastic structure of a non-negative integer-valued autoregressive process. *Journal of Time Series Analysis*, 19(4), 439-455.
- Lee, S., Ha, J., Na, O., and Na, S. (2003). The cusum test for parameter change in time series models. *Scandinavian Journal of Statistics*, 30(4), 781-796.
- Lee, S., Jo, M. (2022). Bivariate random coefficient integer-valued autoregressive models: Parameter estimation and change point test. *Journal of Time Series Analysis*, doi:10.1111/jtsa.12662.
- Mhalla, L., Chavez-Demoulin, V., Dupuis, D. J. (2020). Causal mechanism of extreme river discharges in the upper Danube basin network. *Journal of the Royal Statistical Society Series C*, 69(4), 741-764.
- Nastić, A.S., Ristić, M.M., Bakouch, H.S. (2012). A combined geometric INAR(p) model based on negative binomial thinning. *Mathematical and Computer Modelling*, 55, 1665-72.

- Niu, Y. S., Hao, N., Zhang, H. (2016). Multiple change-point detection: a selective overview. *Statistical Science*, 611-623.
- Page, E.S. (1954). Continuous inspection schemes. *Biometrika*, 41, 100-105.
- Page, E.S. (1955). A test for a change in a parameter occurring at an unknown point. *Biometrika*, 42, 523-527.
- Rissanen, J. (1989). Stochastic Complexity in Statistical Inquiry. Singapore: World Scientific.
- Ristić, M.M., Bakouch, H.S., Nastić, A.S. (2009). A new geometric first-order integer-valued autoregressive (NGINAR(1)) process. *Journal of Statistical Planning and Inference*, 139, 2218-2226.
- Russell, B., Rambaccussing, D. (2019). Breaks and the statistical process of inflation: the case of estimating the ‘modern’ long-run Phillips curve. *Empirical Economics*, 56, 1455-1475.
- Scotto, M.G., Weiß, C.H., Möller, T.A., and Gouveia, S. (2018) The max-INAR(1) model for count processes. *Test*, 27, 850-870.
- Shi, X., Beaulieu, C., Killick, R., and Lund, R. (2022). Changepoint detection: An analysis of the Central England temperature series. *Journal of Climate*, 35(19), 2729-2742.
- Silva, I., Silva, M. E. (2006). Asymptotic distribution of the Yule-Walker estimator for INAR (p) processes. *Statistics and probability letters*, 76(15), 1655-1663.
- Steutel, F.W., Van Harn, K. (1979). Discrete analogues of self-decomposability and stability. *The Annals of Probability*, 7, 893-899.
- Truong, C., Oudre, L., Vayatis, N. (2020). Selective review of offline change point detection methods. *Signal Processing*, 167, 107299.
- Woody, J., Xu, Y., Dyer, J., Lund, R., and Hewaarachchi, A. P. (2021). A Statistical Analysis of Daily Snow Depth Trends in North America. *Atmosphere*, 12(7), 820.
- Yu, G.H., Kim, S.G. (2020). Parameter change test for periodic integer-valued autoregressive process. *Communications in Statistics-Theory and Methods*, 49, 2898-2912.
- Yu, K., Wang, H., Weiß, C.H. (2022). An empirical-likelihood-based structural-change test for INAR processes. *Journal of Statistical Computation and Simulation*, 93, 442-458.
- Zhang, H., Wang, D., Zhu, F. (2010). Inference for INAR(p) processes with signed generalized power series thinning operator. *Journal of Statistical Planning and Inference*, 140, 667-683.
- Zheng, H., Basawa, I. V., Datta, S. (2006). Inference for p th-order random coefficient integer-valued autoregressive processes. *Journal of Time Series Analysis*, 27(3), 411-440.